OPEN ACCESS

ORIGINAL RESEARCH

Mediterranean diet intervention alters the gut microbiome in older people reducing frailty and improving health status: the NU-AGE 1-year dietary intervention across five European countries

Tarini Shankar Ghosh,[1,2] Simone Rampelli,[3] Ian B Jeffery,[1,2] Aurelia Santoro,[4,5] Marta Neto,[1,2] Miriam Capri,[3] Enrico Giampieri,[4] Amy Jennings ,[6] Marco Candela,[3] Silvia Turroni,[3] Erwin G Zoetendal,[7] Gerben D A Hermes ,[7] Caumon Elodie,[8] Nathalie Meunier,[8] Corinne Malpuech Brugere,[9] Estelle Pujos-Guillot,[10] Agnes M Berendsen,[11] Lisette C P G M De Groot,[11] Edith J M Feskins,[11] Joanna Kaluza ,[12] Barbara Pietruszka ,[12] Marta Jeruszka Bielak,[12] Blandine Comte,[10] Monica Maijo-Ferre,[13] Claudio Nicoletti,[13,14] Willem M De Vos,[7,15] Susan Fairweather-Tait,[16] Aedin Cassidy,[17] Patrizia Brigidi,[18] Claudio Franceschi,[19,20] Paul W O'Toole [1,2]

► Additional material is published online only. To view please visit the journal online (http://dx.doi.org/10.1136/gutjnl-2019-319654).

For numbered affiliations see end of article.

Correspondence to
Dr Paul W O'Toole, School of Microbiology, University College Cork APC Microbiome Institute, Cork T12 YN60, Ireland; pwotoole@ucc.ie

TSG, SR, IBJ and AS contributed equally.

Received 16 August 2019
Revised 29 December 2019
Accepted 31 December 2019
Published Online First 17 February 2020

Listen to Podcast
gut.bmj.com

Linked

► http://dx.doi.org/10.1136/gutjnl-2019-320438
► http://dx.doi.org/10.1136/gutjnl-2020-320781

Check for updates

© Author(s) (or their employer(s)) 2020. Re-use permitted under CC BY-NC. No commercial re-use. See rights and permissions. Published by BMJ.

To cite: Ghosh TS, Rampelli S, Jeffery IB, *et al*. *Gut* 2020;**69**:1218–1228.

ABSTRACT

Objective Ageing is accompanied by deterioration of multiple bodily functions and inflammation, which collectively contribute to frailty. We and others have shown that frailty co-varies with alterations in the gut microbiota in a manner accelerated by consumption of a restricted diversity diet. The Mediterranean diet (MedDiet) is associated with health. In the NU-AGE project, we investigated if a 1-year MedDiet intervention could alter the gut microbiota and reduce frailty.

Design We profiled the gut microbiota in 612 non-frail or pre-frail subjects across five European countries (UK, France, Netherlands, Italy and Poland) before and after the administration of a 12-month long MedDiet intervention tailored to elderly subjects (NU-AGE diet).

Results Adherence to the diet was associated with specific microbiome alterations. Taxa enriched by adherence to the diet were positively associated with several markers of lower frailty and improved cognitive function, and negatively associated with inflammatory markers including C-reactive protein and interleukin-17. Analysis of the inferred microbial metabolite profiles indicated that the diet-modulated microbiome change was associated with an increase in short/branch chained fatty acid production and lower production of secondary bile acids, p-cresols, ethanol and carbon dioxide. Microbiome ecosystem network analysis showed that the bacterial taxa that responded positively to the MedDiet intervention occupy keystone interaction positions, whereas frailty-associated taxa are peripheral in the networks.

Conclusion Collectively, our findings support the feasibility of improving the habitual diet to modulate the gut microbiota which in turn has the potential to promote healthier ageing.

Significance of this study

What is already known about this subject?

- Ageing is associated with deterioration of multiple bodily functions and inflammation, leading to the onset of frailty.
- The onset of frailty is associated with changes in the gut microbiota that are linked with a restricted diversity diet.
- The Mediterranean dietary regime is positively associated with health.

What are the new findings?

- Adherence to the Mediterranean diet led to increased abundance of specific taxa that were positively associated with several markers of lower frailty and improved cognitive function, and negatively associated with inflammatory markers including C-reactive protein and interleukin-17.
- These associations were independent of host factors such as age and body mass index.
- Inferred microbial metabolite profiling indicated that the diet-modulated microbiome change was associated with an increase in short/branch chained fatty acid production and lower production of secondary bile acids, p-cresols, ethanol and carbon dioxide.
- Microbiome ecosystem network analysis showed that the bacterial taxa enriched due to the MedDiet intervention occupy keystone interaction positions, whereas frailty-associated taxa are peripheral in the networks.

Gut: first published as 10.1136/gutjnl-2019-319654 on 17 February 2020. Downloaded from http://gut.bmj.com/ on February 17, 2023 by guest. Protected by copyright.

Significance of this study

How might it impact on clinical practice in the foreseeable future?

- Our findings support the feasibility of changing the habitual diet to modulate the gut microbiota which in turn has the potential to promote healthier ageing.
- Our findings also provide a short list of candidate taxa that can be investigated further as live biotherapeutic agents for direct administration to older subjects to reduce the onset of frailty.

INTRODUCTION

Frailty that accompanies ageing involves failure of multiple physiological systems[1] and a persistent activation of the innate immune inflammatory response.[2] Frailty may include the development of chronic low-grade inflammation (ie, inflammageing),[3] loss of cognitive function,[4] sarcopenia[5] and the development of chronic diseases like diabetes and atherosclerosis.[3] Modification of dietary patterns such as adopting a Mediterranean diet (MedDiet) has been suggested as a major therapeutic strategy to address frailty.[6] The MedDiet regimen is characterised by increased consumption of vegetables, legumes, fruits, nuts, olive oil and fish and low consumption of red meat and dairy products and saturated fats.[7] Adherence to a MedDiet is associated with reduced mortality, increased antioxidant activity, reduced incidences of several diseases, as well as reduced inflammation.[8] Several studies have shown that increased adherence to the MedDiet is linked to reduced frailty.[9] Beyond the negative association with disease, higher level adherence to the MedDiet has been associated with beneficial changes in gut microbiome composition, with reduction in proteobacterial abundance accompanied by increased levels of short chain fatty acid production.[10 11] On a global basis, the majority of elderly people do not consume a MedDiet and, in fact, a major challenge in elderly healthcare is the consumption of a restricted diet which is associated with a low-diversity gut microbiome, especially in subjects in long-term residential care.[12 13] In previous work we have used fine detail bioinformatic (bi-clustering) analysis to identify specific microbial taxa that are lost in incremental stages in the transition from high-diversity microbiome healthy subjects to low-diversity frail subjects.[14] In a recently completed 6-month dietary intervention in which elderly individuals were supplemented with up to 20 g daily of five prebiotics, multiple gut microbial taxa responded to the prebiotic supplementation,[15] but there was no change in overall microbiota alpha diversity and trends towards a reduction of inflammatory markers did not reach overall statistical significance. We thus reasoned that a more dramatic dietary intervention was required.

The NU-AGE dietary intervention project aimed to study the effect of the administration of a customised MedDiet for 12 months in a large cohort of more than 1200 elderly individuals aged 65–79 years,[16] distributed across five different countries (Poland, Netherlands, UK, France and Italy). Baseline and post-intervention results from this study have reported gender- and country-specific differences for measured metabolite levels as well as body composition data. A significant association was observed between increased adherence to the NU-AGE MedDiet and enhanced global cognitive ability and episodic memory.[17] Moreover, higher adherence has been shown to reduce the rate of bone loss in individuals with osteoporosis[18] and to improve innate immune function,[19] blood pressure and arterial stiffness.[20]

In the current study we have profiled the effect of the NU-AGE MedDiet on the gut microbial community of a subset of participants from the NU-AGE trial comprising 612 individuals (289 controls (145 men and 144 women) and 323 with the NU-AGE MedDiet (141 men and 182 women)). A variety of beneficial outcomes were correlated to microbiome alterations.

METHODS

Study participants and dietary intervention

The NU-AGE study is a 1-year, randomised, multicentre, single-blind, controlled trial (registered with clinicaltrials.gov, NCT01754012). Details on the recruitment of participants and the dietary intervention and the collection of metadata corresponding to anthropometry, frailty and cognitive response have been previously described.[17 21] Online supplementary table 1 provides descriptive statistics of participants by country for whom paired microbiome profiles at baseline and the final time point were available.

Measurement of inflammatory and adiposity related hormones

Methods for the measurements of inflammatory markers have been previously described.[22] Online supplementary text 1 briefly summarises the techniques used for this purpose.

DNA extraction and 16S rRNA gene sequencing

Microbial DNA was extracted from stool samples using the repeated bead beating method as previously described,[23] with some modifications.[24] The detailed protocol adopted for the DNA and 16S rRNA gene sequencing is described in online supplementary text 2.

Bioinformatic and biostatistical analysis

Online supplementary text 3 provides a complete description of the methodology used for the bioinformatics and the multivariate statistical analysis of the amplicon sequence data. This includes preprocessing of sequenced reads,[25] identification of and removal of chimaeras,[26 27] taxonomic classification of Operational Taxonomic Units (OTUs),[28 29] machine learning-based identification of microbiome taxa associated with the dietary intervention[30] (described in online supplementary figure 1), identification of taxonomic modules using the iterative Binary Bi-clustering of Gene-sets (iBBiG) approach,[31] association analysis of dietary adherence and diet-associated taxonomic markers with the various components of diet as well as with the markers of frailty and inflammation, computation of MedDiet-associated microbiome indices (described pictorially in online supplementary figure 2) and the association analysis of these indices with dietary components, inflammation and frailty, obtaining inferred metabolite profiles based on per-sample species abundances and previously curated mappings of experimentally validated species-to-metabolite links[32 33] and generation and visualisation of co-occurrence networks and computation of centrality measures (see online supplementary text 3).[30 34]

RESULTS

Diet and microbiome profiles co-vary and differ between countries at baseline

Overall, there were 612 individuals (across the control and intervention cohorts) for whom paired microbiome data were collected at both the baseline and 1 year (referred to as 'final') time points. While the age ranges of the individuals in the control and intervention cohorts across countries were similar, there was

Gut: first published as 10.1136/gutjnl-2019-319654 on 17 February 2020. Downloaded from http://gut.bmj.com/ on February 17, 2023 by guest. Protected by copyright.

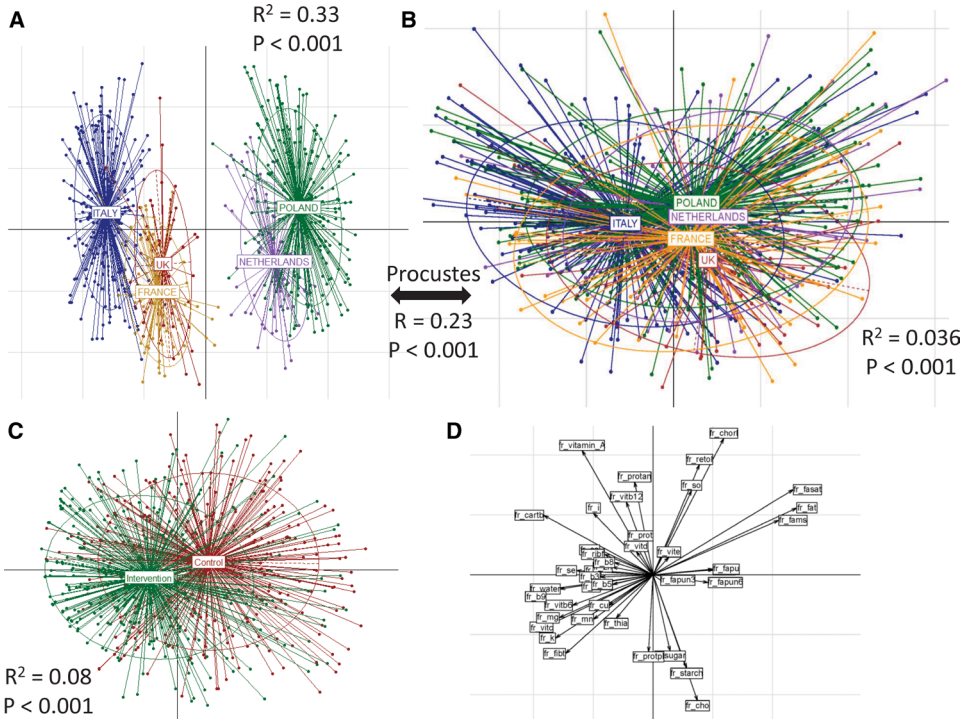

Figure 1 Baseline habitual diet and microbiota composition separate and co-vary by country, and the dietary intervention altered macronutrient profiles. Principal component analysis (PCoA) plots of (A) baseline dietary profiles and (B) baseline 16S microbiome profiles across the five different countries. For both, the PERMANOVA p values showing the significance of the association with the countries are also indicated. For the association between the dietary frequencies, the microbiome profiles, R^2 and the significance values obtained using the Procrustes analysis are also shown. The results indicate that there are country-specific patterns in dietary habits which are also reflected in the microbiome profiles. (C) PCoA plots showing the distinct variations in the dietary patterns in the intervention and control cohorts. The PERMANOVA p values of these differences are also indicated. This reflects the effect of the dietary intervention to detect the specific dietary components driving these effects. Associations were computed between the intake frequencies of the components and the two PCoA axes (PCoA1 and PCoA2). These associations are plotted in (D). While the intervention group is primarily driven by an increase in consumption of fibres, vitamins (C, B6, B9, thiamine) and minerals (Cu, K, Fe, Mn, Mg), the changes in controls are associated with an increase in fats consumption.

a marginally higher representation of women in the intervention cohort (Fisher's test p<0.12; online supplementary table 1). Principal coordinate analysis (PCoA) indicated significant dietary differences at baseline between the countries showing three distinct subgroups (figure 1A) (PERMANOVA p<0.001: R^2=0.33): the first containing Italian subjects; the second containing UK and French subjects; and the third containing those from the Netherlands and Poland. This specific pattern of clustering was also observed at the level of PCoA (based on Spearman distances) using the 16S rDNA OTU profiles at baseline (figure 1B) (significant: PERMANOVA p<0.001; although with considerable overlaps: R^2=0.036). While the Italian subjects had a distinct microbiome composition, those from UK/France and Poland/Netherlands were more like each other. Procrustes analysis of the food consumption and the OTU abundance profiles confirmed a significant association between diet and microbiome composition (figure 1A,B; online supplementary figure 3; Procrustes RV coefficient 0.23; p<0.001). Specific microbiome components drove country-specific separations at baseline (Mann–Whitney test FDR-corrected p<0.15; online supplementary figure 4A–B). As expected, the dietary variations within the intervention group were significantly different from the control group (envfit p<0.006) (figure 1C). These changes in the intervention group were primarily driven by an increase in the intake of fibres, vitamins (C, B6, B9, thiamine) and minerals (Cu, K, Fe, Mn, Mg), while changes in the controls were associated with an increase in fat intake (saturated fats and mono-unsaturated fatty acids) relative to the MedDiet intervention group (figure 1D).

Increasing adherence to the NU-AGE MedDiet influences specific components of the gut microbiome previously associated with health

There were no significant changes in the global gut microbiota diversity in the subjects from individual countries in the intervention and control groups (online supplementary figure 5). However, we observed that, across the study, increasing adherence to the diet was associated with an attenuated loss of microbiome diversity (table 1). For a finer detailed microbiota–diet association analysis, we used adherence scores to the MedDiet, previously calculated based on the NU-AGE Food Based Dietary Guidelines (FBDG).[35] These are recommendations that act as the basis for facilitating or measuring adherence to healthy eating initiatives or dietary interventions for improving public health. The NU-AGE FBDG covered 15 dietary goals including a vitamin D supplement that has been described in detail by Berendsen *et al*.[35] We created Random Forest (RF) models to predict dietary adherence from microbiome profiles at both the baseline and final (1-year) time points. For both models, the correlations observed between the predicted food score (using the Random Forest model) and the actual food score were significant (baseline: R=0.27; p<1.2e-11; final: R=0.30; p<2.2e-14) (online supplementary figure 6A,B), indicating that there was a clear association between the microbiome and adherence to

Gut: first published as 10.1136/gutjnl-2019-319654 on 17 February 2020. Downloaded from http://gut.bmj.com/ on February 17, 2023 by guest. Protected by copyright.

Table 1 High adherence to a MedDiet attenuates the loss of diversity of the gut microbiome

	Low adherence				Medium adherence				High adherence			
	Estimate	Standard error	Z value	P value	Estimate	Standard error	Z value	P value	Estimate	Standard error	Z value	P value
Intercept	387.11	113.53	3.41	0.00065***	283.04	117.05	2.42	0.016*	412.97	97.48	4.24	2.3e-5**
Time point	−9.51	4.85	−1.96	**0.049***	−9.34	4.99	−1.87	**0.061**(.)	−3.84	4.93	−0.78	**0.44**
Gender	-2	12.34	−0.16	0.87	16.97	12.62	1.34	0.179	−7.40	10.93	−0.68	0.5
Age	−0.19	1.57	−0.12	0.90	1.21	1.64	0.74	0.46	−0.54	1.37	−0.39	0.69

A significant decline in diversity was observed across the time points in the low adherence group (as indicated in the estimate value).
Data tabulated are from regression analysis of the change in gut microbial diversity across the time points (baseline vs final), taking age and gender as the confounders in the three adherence change groups.
The decline attenuated from being marginally significant in the medium adherence group to non-significant in the high adherence group. Please refer to the Methods section for the definition of 'low', 'medium' and 'high' adherence groups of individuals.
The notations used for the p-values of significance are **P < 0.01; *P < 0.05 and; ***P < 0.10

the MedDiet. For either time point, an optimal set of 75 OTUs provided the highest predictive performance (a total number of 129 OTUs combining both; see online supplementary figure 6C,D) to identify the microbiome response to the MedDiet. We refer to these as 'diet-responsive' OTUs/taxa/markers throughout this study. Overall, using this optimal set of OTUs, the correlation between the predicted and the observed adherence score was 0.39 (p<2.2 e-16) (figure 2A). The list of the top predictive

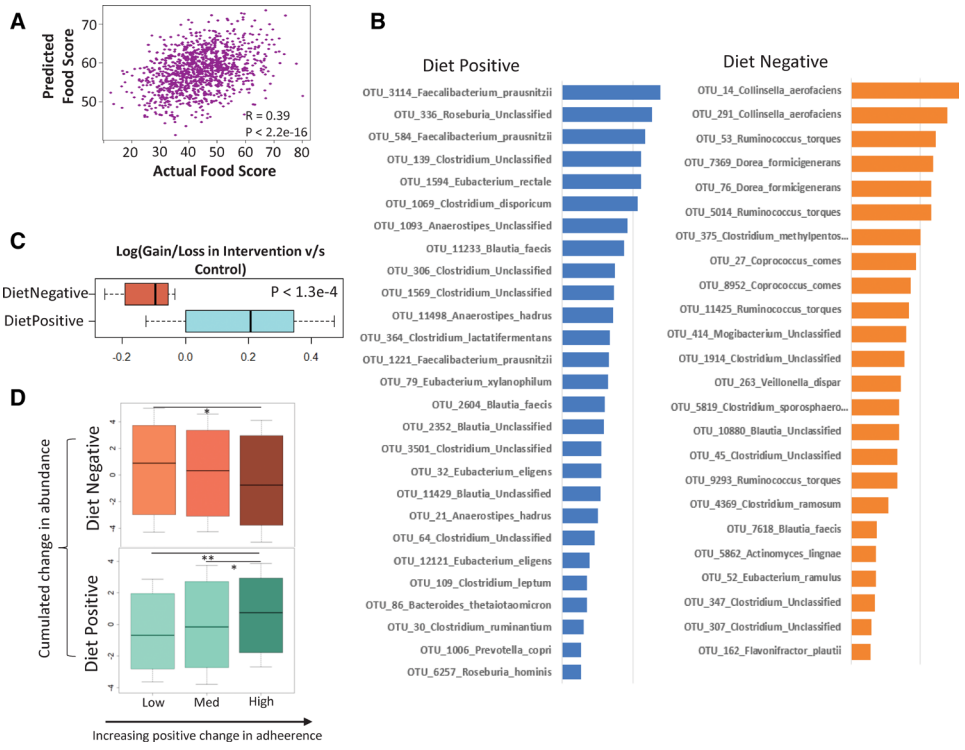

Figure 2 Identification of diet responsive taxa by machine learning. (A) Correlation between the actual and predicted diet scores obtained using the random Forest approach. (B) Ranked feature importance scores of the top marker Operational Taxonomic Units (OTUs) responding positively and negatively to diet, along with their taxonomic affiliations (see Methods section for the selection of the top markers significantly associated with the food score). Top markers having a significant positive or negative association with diet scores were tagged as 'DietPositive' and 'DietNegative', respectively. The two groups show distinct taxonomic classifications. While DietPositive markers have an over-representation of species like *Faecalibacterium prausnitzii*, *Eubacterium* and *Roseburia*, DietNegative markers are characterised by the presence of *Ruminococcus torques*, *Collinsella aerofaciens*, *Coprococcus comes*, *Dorea formicigenerans*, *Clostridium ramosum*. The associations of the different groups with the adherence scores are also reflected in the changes across the time points between the intervention and control cohorts (as shown in C). (C) Boxplot showing the log-fold change in the gain/loss ratios of the various taxa (ie, the number of individuals in which a given OTU is increased divided by the number of individuals in which it is decreased across the time points) in the intervention cohorts compared with non-intervention in the two groups. While the DietPositive OTUs had a relatively positive increase in the intervention cohort (compared with the non-intervention group), changes in the DietNegative indicated a significant decrease with the intervention. (D) Boxplots showing the variation in the across time point changes in the DietPositive and the DietNegative OTUs in groups of individuals obtained after dividing them into three tertile groups (low, medium and high) based on increasing positive changes in adherence to the NU-AGE diet. The p values of the significance of the association are indicated as ****p<0.0001, ***p<0.001, **p<0.01 and *p<0.05.

Gut: first published as 10.1136/gutjnl-2019-319654 on 17 February 2020. Downloaded from http://gut.bmj.com/ on February 17, 2023 by guest. Protected by copyright.

OTUs along with their taxonomic classification (obtained using SPINGO[28]) is provided in online supplementary table 2.

A total of 44 top predictive OTUs had a positive association with adherence scores (enriched with increasing adherence to diet) and 45 had a negative association (depleted with MedDiet adherence) (see Methods section). We refer to these as 'Diet-Positive' and 'DietNegative' OTUs, respectively. A subset of these OTUs (with defined taxonomic classifications) along with their absolute feature importance scores is shown in figure 2B. The sets of taxa comprising these two groups are distinct. The DietPositive OTUs were mainly assigned to *Faecalibacterium prausnitzii*, along with *Roseburia* (*R. hominis*), *Eubacterium* (*E. rectale*, *E. eligens*, *E. xylanophilum*), *Bacteroides thetaiotaomicron*, *Prevotella copri* and *Anaerostipes hadrus*. A majority of these taxa have previously reported positive health associations including production of short chain fatty acids (SCFAs) and anti-inflammatory properties as well as negative associations with diseases like type 2 diabetes and colorectal cancer.[36–38] *F. prausnitzii* had also been negatively associated with frailty onset in the elderly.[39] In contrast, the DietNegative OTUs mainly belonged to *Ruminococcus torques*, *Collinsella aerofaciens*, *Coprococcus comes*, *Dorea formicigenerans*, *Clostridium ramosum*, *Veillonella dispar*, *Flavonifractor plautii* and *Actinomyces lingnae*. Increase in the abundances of *R. torques*, *C. aerofaciens*, *C. ramosum* and *V. dispar* have been associated with type 2 diabetes and colorectal cancer, atherosclerosis, cirrhosis and inflammatory bowel disease.[38 40–43] These findings collectively suggest that adherence to the MedDiet has the potential to modulate the microbiome in a direction positively associated with health.

Notably, in spite of country-specific microbiome composition differences at baseline (figure 1B; online supplementary figure 4A,B) and different dietary adherences (online supplementary figure 7A) (as also reported by previous studies on this cohort),[35 44] the diet-responsive taxa identified across the entire cohort were largely shared across the different nationalities—that is, their association with diet was not specific for any country (see online supplementary text 4; online supplementary figure 4A,B; online supplementary figure 7). Their associations with MedDiet adherence were further validated by their pattern of abundance variation in both the intervention and control cohorts, as well as in individuals ranked by increasing adherence to the diet (see online supplementary text 5; online supplementary figure 8, figure 2C,D).

Next we investigated the co-occurring modules within the gut microbiomes. These modules are analogous to 'guilds' within the microbiomes that have similar or associated functional properties. We used iBBiG to identify modules in the gut microbiome,[31] an approach we previously used to identify granular differences in the microbiome as a function of healthy ageing in the ELDERMET cohort[14] (see online supplementary text 3; online supplementary figure 9; online supplementary tables 3 and 4). iBBiG identified six overlapping taxonomic modules (named A to F) within the NU-AGE dataset. Notably, we identified a specific module C which was significantly over-abundant in individuals with increased frailty and also increased in representation in the set of DietNegative OTUs (see online supplementary text 6; online supplementary figure 9C,D). This indicates that module C is similar to the long-stay-like modules we identified in ELDERMET individuals.[14] However, the specific enrichment of module C in the set of OTUs depleted with MedDiet adherence indicated the likelihood that the MedDiet successfully modulated the gut microbiome in a manner negatively associated with frailty.

Adherence to the NU-AGE MedDiet intervention modulated the microbiome in a manner negatively associated with frailty and inflammation

A major objective of the NU-AGE dietary intervention was reduction of frailty and inflamm-ageing. The study subjects were categorised into Non-Frail (or apparently healthy), Pre-Frail and Frail groups based on Fried scores.[21] While the DietNegative taxa showed a stepwise significant decrease with the three frailty groupings (ie, Frail>Pre-Frail>Non-Frail), DietPositive taxa showed a significantly higher abundance in healthy (Non-Frail) individuals compared with Frail individuals (see online supplementary figure 10A). The DietPositive taxa showed a significantly positive change in individuals with reduced frailty (see online supplementary text 7; online supplementary figure 10B). During the intervention period, within the control cohort there was a marginally significant increase in the proportion of individuals with increased frailty (compared with the intervention group) (Fisher's test $p<0.06$; online supplementary figure 10C). However, we could not observe a direct association between dietary adherence scores and frailty (online supplementary figure 10D). We hypothesised that the effect of dietary adherence on frailty could be indirect, whereby increasing adherence to a Mediterranean diet could modulate the microbiome (potentially with some non-responders), and that this microbiome response could have a direct association with an attenuation of, or reduced risk of, frailty and improvements in other measures of well-being.

To investigate this, we computed the associations between the diet-responsive OTU markers and specific indices of frailty, cognitive function and inflammation across the entire study cohort (see online supplementary table 5 for list of metadata tested). The objective was to test if diet-responsive taxa showed significantly different trends of association with these indices (see online supplementary figure 11). Overall, although the absolute values of the associations were relatively weak, we observed significant differences in the association patterns of DietPositive and DietNegative OTUs for five different cytokines/biomarkers (namely, pro-inflammatory high-sensitivity C reactive protein (hsCRP) and interleukin 17 (IL-17), anti-inflammatory sGP130 as well as adiponectin and leptin); three frailty-associated measures (Fried Score, Hand Grip Strength and Gait Speed Time); BabCock Memory Score and Constructional Praxis (both associated with cognitive function). The most notable observation, however, was the pattern of these associations. The DietPositive OTU markers had consistent negative associations (significantly lower than the DietNegative markers) with the inflammatory markers hsCRP and IL-17 levels as well as with Fried Scores and Gait Speed Time (both measures associated with increased frailty) (figure 3A). In contrast, their associations were consistently positive with measures of improved cognitive function (eg, Constructional Praxis, BabCock Memory Score), reduced frailty (Hand Grip Strength) and two of the cytokines (adiponectin and sGP130) (a trend exactly opposite to that for DietNegative OTU markers). While the role of adiponectin as an anti-inflammatory marker is well documented,[45] sGP130 is a negative regulator of the pro-inflammatory trans IL-6 signalling pathway.[46] Notably, in spite of the country-specific variations in dietary intake, microbiome scores and adherence scores, each of these associations (with the exception of BabCock Memory Scores) could be replicated (both in terms of direction as well as the significance of the associations) in at least three of the countries (six of the 10 associations replicated in four of the five countries) (figure 3B). These results clearly indicate that

Gut: first published as 10.1136/gutjnl-2019-319654 on 17 February 2020. Downloaded from http://gut.bmj.com/ on February 17, 2023 by guest. Protected by copyright.

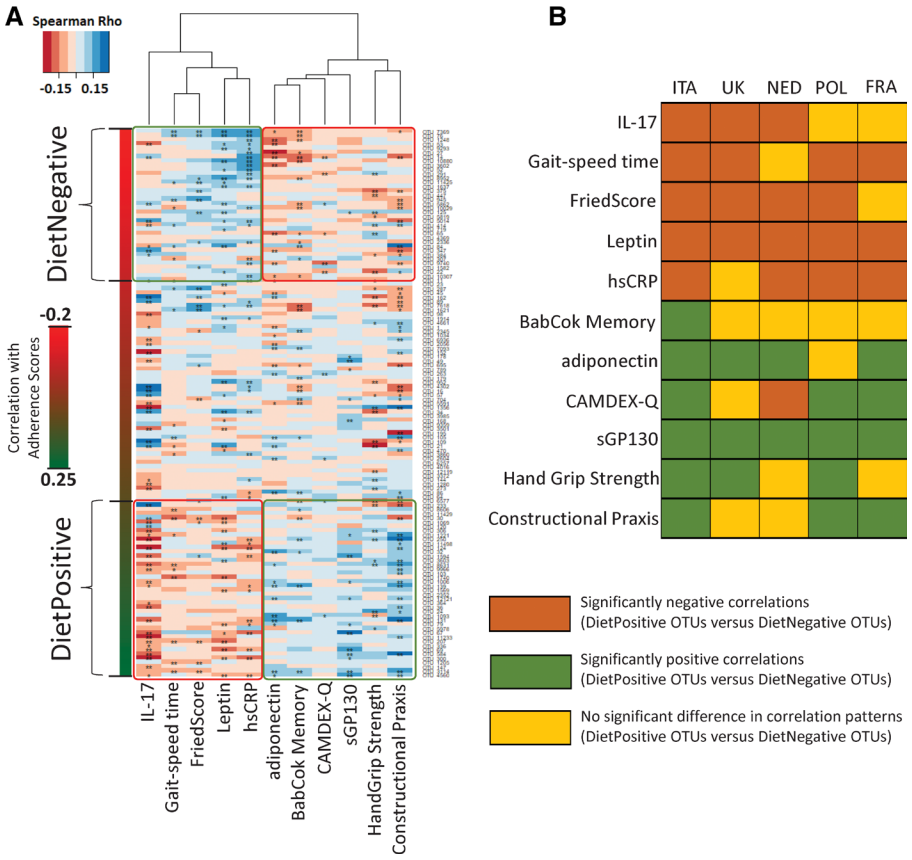

Figure 3 Consistent association of diet responsive taxa with different measures of frailty, cognitive function and inflammation. (A) Heatmap showing the variation of the association patterns (obtained using Spearman rhos) of the adherence associated marker Operational Taxonomic Units (OTUs) (arranged from top to bottom in increasing order of their correlations with the adherence scores) with the selected measures of frailty, cognitive function and the pro/anti-inflammatory cytokine levels. For each cell, colours indicate the Spearman rho values (as shown). **Significant association with FDR-corrected p value <0.15. *Marginal association with nominal p value <0.05. The DietPositive and DietNegative OTUs are also demarcated. Specific differences could be observed between the association pattern of the different measures and the DietPositive and DietNegative OTUs. For certain measures such as high-sensitivity C reactive protein (hsCRP) levels, interleukin 17 (IL-17) levels and gait speed time, DietPositive OTUs were observed to have significantly more negative correlations as compared to DietNegative OTUs. For the other measures associated with reduced frailty and improved cognitive function, as well as adiponectin and sGP130 levels, an exact opposite trend was observed. (B) Heat plot showing the replication of these trends individually within each of the country-specific cohorts. Brown indicates those cases where the correlations of the DietPositive OTUs were significantly more negative than the DietNegative group, green indicates those cases with the opposite trend and yellow indicates those cases of no significant change.

adherence to the NU-AGE MedDiet is associated with modulation of the microbiome in a manner that is relatively consistent (across the countries) and is in turn associated with reduced frailty, improved cognitive function and reduced inflammation.

Microbiome response, accompanied by specific beneficial changes in the gut metabolic profiles, is the key intermediate between dietary adherence and health

Based on the preceding findings, it seemed likely that a microbiome associated with dietary adherence was more important for improved health status than merely adherence to the diet itself. Testing this hypothesis required the computation of measurable 'microbiome scores/indices' (analogous to the dietary adherence scores) that would take into account the variations associated with individual marker OTUs. Switching to the NU-AGE MedDiet is characterised by changes in the consumption pattern of specific dietary components—namely, an increase in the consumption of fibres (vegetables, fruits), carbohydrates (wholegrains), plant proteins (legumes), polyunsaturated fatty acids (fish) and vitamins such as vitamin C (fruits) and a concomitant decrease in the consumption of fats, alcohol, sodium and sugar (sweets).[35]

We first validated the diet-responsive OTUs (identified based on their association with the overall NU-AGE FBDG scores) by checking their associations with the consumption patterns with the different food components (partial Spearman correlations taking into account age, body mass index, gender, country and polypharmacy as confounders). We observed that OTU markers with an increasing positive association with FBDG adherence scores showed increasing positive correlations with fibre, vitamin C, vitamin D, plant proteins and carbohydrates and increasing negative associations with the components alcohol, fats and sugar whose consumption was decreased during the MedDiet change[35] (see online supplementary figure 12). Thus, the above results indicate that the associations of the marker OTUs were not only with the overall FBDG scores, but also with individual dietary components whose modulations were associated with the NU-AGE MedDiet intervention (even after taking into account all host-associated confounding factors like age, body mass index, gender, country and polypharmacy). This validated the association of the dietary markers with the dietary intervention. Further, each of the diet-responsive OTUs had a specific degree of correlation with the dietary adherence scores

Gut: first published as 10.1136/gutjnl-2019-319654 on 17 February 2020. Downloaded from http://gut.bmj.com/ on February 17, 2023 by guest. Protected by copyright.

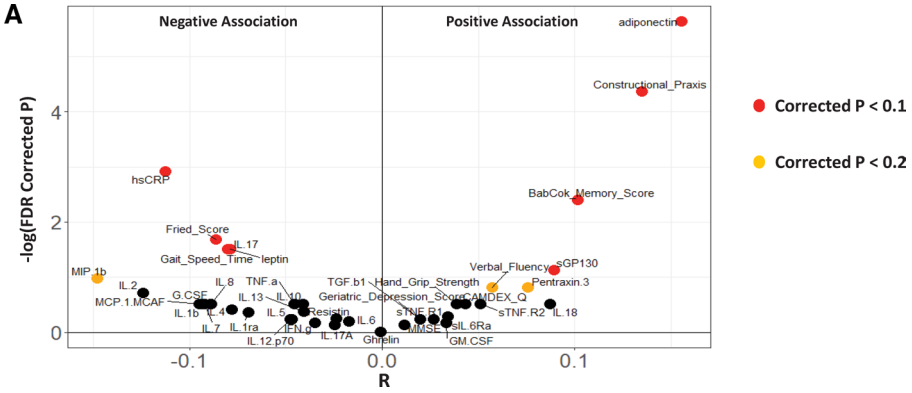

Figure 4 MedDiet microbiome index correlates with reduced frailty, improved cognitive function and reduced inflammation, independent of the adherence scores. Violin plot showing the association (partial Spearman correlations) of the different measures of frailty, cognitive function and inflammatory marker levels with the MedDiet-modulated microbiome index after taking into account the adherence scores as a confounder. The x axis shows the Spearman rho values and the y axis indicates the −log (base 10) of the p values. Most negatively associated measures are expected to be at the extreme left of the plot, the most positively associated measures are expected to be at the extreme right of the plot. Points are coloured based on the significance of the obtained associations (red indicates associations with FDR-corrected p<0.1, orange indicates associations with FDR-corrected p<0.2). The MedDiet microbiome index is observed to be associated with several measures associated with reduced frailty, reduced inflammation and improved cognitive function and this association is independent of the adherence scores.

and specific trends of association with the dietary components (see online supplementary figure 12). Based on the overall correlations of the diet-associated marker OTUs with the adherence scores as well as the abundances marker OTUs in a given sample, we calculated a sample-specific diet-modulated microbiome index (see Methods section; online supplementary figure 2). As expected, the microbiome index was positively correlated with the overall adherence scores and also captured the overall association patterns of the individual marker OTUs (ie, positive associations with fibre, carbohydrate, plant proteins, vitamin C, polyunsaturated fatty acids and negative associations with fats, alcohol and sugar), indicating its validity as a proxy for the taxonomic markers associated with consumption of the MedDiet (see online supplementary figures 12,13; online supplementary text 8).

We then checked the association of this index with the different measures of frailty, cognitive function and inflammation (across the entire cohort), considering the adherence scores as a confounder. Ten of the 11 associations with measures of improved cognition, reduced frailty and inflammation could be reproduced. We also observed additional negative associations with the inflammation-related cytokines interleukin (IL)-2 and macrophage inflammatory protein (MIP)-1b, and positive associations with verbal fluency (figure 4). These results show that the diet-modulated microbiome components are associated with frailty, inflammation and cognitive function independent of the adherence scores (ie, these are not indirect consequences of associations with dietary adherence). We had previously shown that these associations were stable across the different countries (figure 3B). We next checked the effect of confounders (such as age, body mass index, gender, disease pathophysiologies and medication intake) on the extent of diet–taxon associations. Individuals with multiple diseases, specifically those with diabetes, heart attack and inflammatory disorders, were observed to have significantly lower microbiome scores compared with non-diseased controls (lower but marginally significant for cancer) (see online supplementary figure 14A–E; online supplementary text 9; online supplementary table 6). However, the pattern of association of the microbiome index with seven of the 10 inflammatory markers and frailty indices (identified in figure 4) largely remained invariant, even after taking into account all confounders including age, body mass index, gender, polypharmacy and different disease pathophysiologies (see online supplementary text 9; online supplementary figure 15).

Even with respect to the across time point changes, while change in dietary adherence scores were significantly associated with change in the microbiome index, it was the change in the microbiome index that was positively associated with improvement in cognitive function, physical well-being and negatively associated with inflammatory markers like hsCRP (see online supplementary text 10; online supplementary figure 16). Positive changes in microbiome indices were also associated with positive changes in the levels of the anti-inflammatory cytokine IL-10 and negative changes in the ratio of hsCRP to anti-inflammatory cytokine levels, further indicating the negative association of the diet-associated microbiome index with inflammatory cytokine levels (see online supplementary figure 16C and online supplementary text 10).

The positive influence of the diet-modulated microbiome change on health status is likely to be driven by specific microbial metabolites. Given that faecal metabolomic data were unavailable for the individuals, we predicted the functional metabolic profiles of the gut microbiome using the corresponding 16S species composition profiles (see Methods section). Correlating the across time point changes in the abundances of these predicted metabolic profiles with the microbiome index change identified dramatic differences across the microbiome response landscape (see online supplementary figure 17). A positive microbiome change was associated with an increase in the microbial consumption of fibre-associated non-starch polysaccharides (probably indicative of Mediterranean diet change). In contrast, a negative change was associated with an increase in microbial simple sugar consumption. A negative microbiome response was also accompanied by a predicted increase in the microbial consumption of tauro- and glyco- derivatives of bile acids (such as taurocholate or glycochenodeoxycholate) to secondary bile acids (lithocholate, deoxycholate) through cholate and chenodeoxycholate (see online supplementary figure 18A). Bile acid dysregulation is associated with different disease conditions,[47] specifically the increase in production of lithocholic and

Gut: first published as 10.1136/gutjnl-2019-319654 on 17 February 2020. Downloaded from http://gut.bmj.com/ on February 17, 2023 by guest. Protected by copyright.

deoxycholic acid has been associated with colorectal cancer.[48] In contrast, increased production of both branched chain fatty acids (BCFAs) and SCFAs are associated with a positive microbiome response. A positive association of SCFAs with host health is well recognised.[49] Previous studies measuring the metabolomic changes associated with intake of a MedDiet have also observed a similar increase in SCFA levels,[10 50] as well as an exactly similar link wherein MedDiet-like dietary modulations (increased fibre intake and decreased fat intake) were observed to be positively associated with faecal SCFA levels and negatively associated with faecal secondary bile acids.[51 52] Furthermore, in the current study we had data for the measured plasma levels of cholic acid (CA), glycochenodeoxycholic acid (GDCDA) and chenodeoxycholic acid (CDCA) for a subset of individuals belonging to the Italian and Polish cohorts. For GCDCA and CDCA, correlating the plasma levels of these bile acids with the abundances of the diet-associated markers revealed trends that the DietPositive OTUs had significantly more positive associations with GCDCA levels and more negative associations with CDCA levels compared with DietNegative OTUs (online supplementary figure 18B). By grouping this subset of individuals into three terciles based on their GDCDA/CDCA ratios, we observed that individuals with an increasing GCDCA/CDCA ratio were associated with a significantly positive change in their diet-associated microbiome index (online supplementary figure 18C). These results confirm the predicted metabolite profiles wherein individuals with increasing diet-associated microbiome indices were predicted to have decreased microbial conversion of GDCDA to CDCA (and thereafter to lithocholic acid (LCA) and deoxycholic acid (DCA)), thereby resulting in higher GDCDA/CDCA levels. Thus, some of the key global changes (in bile acid and SCFA levels) we detect and that we predicted to be linked with diet-associated microbiome response have been reported in the literature across multiple studies as well as the plasma level analysis. The only conflicting trend was with CA levels which were observed to show the pattern opposite to that expected. However, it could be because the measurements were on serum samples (in contrast to faecal levels) and CA/CDCA are produced by both the liver and the microbiota (see online supplementary figure 18C).

A negative microbiome response was also associated with other detrimental metabolites like p-cresol, ethanol and carbon dioxide, whose relative overproduction is associated with onset of colorectal cancer, insulin resistance, non-alcoholic fatty liver disease, cytotoxicity and small intestinal bacterial overgrowth.[53–57] Notably, at baseline the diet-associated microbiome index was observed to be negatively associated with multiple diseases including hypertension, diabetes and cancer (online supplementary figure 14). Thus, although inferred rather than measured, the data indicate that metabolic change associated with a positive microbiome response beneficially impacts host health.

DietPositive OTUs are keystone species in the gut microbial community

Finally, we evaluated the role of the diet-responsive taxa in the overall microbiome community structure, represented by networks defined by the Reboot Approach (see Methods section).[30] A co-occurrence network provides a representation of nodes and edges (interconnecting lines) between these nodes, wherein the nodes represent the taxa (in this case, the OTUs) and the edges between the nodes represent a significant co-occurrence relationship between them (across a provided set of observations or samples). The placement of the taxa within a co-occurrence network indicates the relative importance of the taxa in the stability of the community. We first obtained the co-occurrence network for all the samples across time points for both cohorts. The major component of the co-occurrence network is a conglomeration of clusters of taxa, with other taxa acting as interlinking hubs. However, the positioning of the majority of DietPositive and DietNegative taxa was strikingly different. The DietPositive taxa were either located centrally at the hubs of the network or as linking nodes within the major subnodes (figure 5A). This shows the centrality of these taxa in the gut community structure, a phenomenon termed 'keystone species'.[58] In contrast, the majority of the DietNegative taxa were placed at the periphery of the network. We probed this observation by computing two centrality measures for each taxon in the network: 'degree centrality', which is the number of nodes connected to a given node, and 'betweenness centrality', which is the number of paths connecting any two nodes that pass through a given node. DietPositive taxa had a significantly higher degree of betweenness centrality compared with the DietNegative taxa or the non-associated markers (figure 5B,C). We regenerated the network within each of the different countries as well as across overlapping windows of samples of increasing dietary adherence (see online supplementary figure 19; online supplementary figure 20; online supplementary figure 21A). Despite major differences in the overall structure of the individual networks, the placement patterns of the taxa as well as their relative importance within the gut microbial networks were invariant irrespective of the country. The DietPositive taxa had significantly higher centrality measures irrespective of the nationality and the dietary adherence of the individuals. As expected, there were also distinct patterns of interactions for the DietPositive and DietNegative groups of taxa, specifically with respect to the iBBiG identified frailty-associated module C, which had negative co-occurrence propensities with the DietPositive group (figure 5D). Interestingly, the strength of the co-occurrence propensities became significantly more negative with increasing adherence to the diet (figure 5E). This was not observed for any of the other taxonomic modules (see online supplementary figure 21B).

DISCUSSION

The current results provide a systemic view of the effect of consuming the NU-AGE MedDiet on the microbiome and subsequently on biomarkers of health in the elderly. A significant challenge for the current study was the high level of microbiome variability across individuals in five countries, resulting in a low signal-to-noise ratio which translated to weaker taxonomic signals for association with metadata. Analysis using traditional methodologies are useful and provide statistical rigour, even if the assumption of independent variables is not a true reflection of the community structure in the microbiota. However, due to the multitude and disparate nature of the microbiota structure configurations across individuals, combined with the relatively small effect of diet over a year of life in an established gut microbiota community as well as other aspects such as the subjective nature of the dietary measurements that is expected for community-dwelling individuals and the assumption that dietary measurements accurately measure the actual dietary change, the traditional statistical methodologies are unable to identify the taxa associated with the statistically significantly lower loss of diversity associated with adherence to the MedDiet. To establish the diet-responsive taxa and generate a diet-associated microbiome index, we applied a novel leave-one-out-cross-validation machine-learning methodology to predict the adherence score for each individual with good accuracy and used these predictive

Gut: first published as 10.1136/gutjnl-2019-319654 on 17 February 2020. Downloaded from http://gut.bmj.com/ on February 17, 2023 by guest. Protected by copyright.

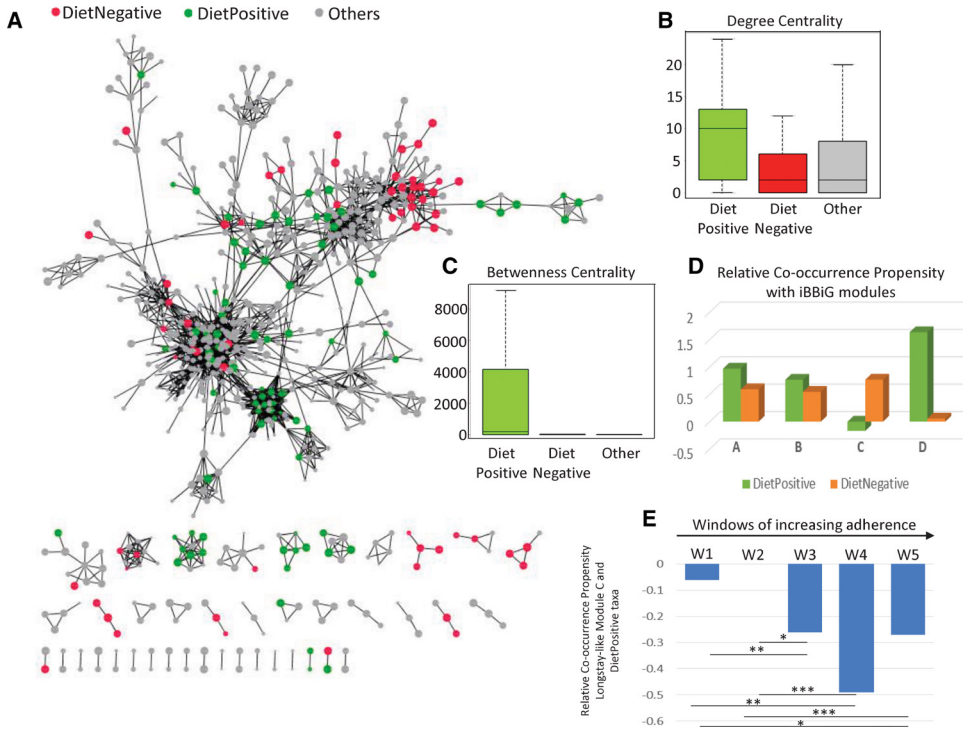

Figure 5 Bacterial taxa that respond positively to Mediterranean diet intervention occupy keystone interaction nodes for peripheral frailty-associated taxa in microbiome networks. (A) Representation of the Operational Taxonomic Unit (OTU) co-occurrence network obtained for all the samples across the time points and cohorts with the DietPositive, DietNegative and non-correlated OTUs shown in green, red and grey colours, respectively. The network shows two distinct characteristics of the DietPositive and DietNegative markers (or OTUs). While the DietNegative markers (barring a few exceptions) are observed to occur as the peripheral nodes in the network, the DietPositive markers mostly act as either the centrally connected hub nodes or as interconnecting nodes between the hubs, indicating their centrality to the microbiome. This is also reflected in the comparison of the degree and betweenness centrality measures shown as boxplots in (B) and (C), respectively. (D) Relative co-occurrence propensity (calculated as the logged ratio of the number of positive edges to the number of negative edges) between the DietPositive and DietNegative OTUs with those belonging to the different iterative Binary Bi-clustering of Gene-sets (iBBiG) modules. It was observed that, specifically for the frailty-associated longstay-like module C, while the DietNegative markers showed a positive co-occurrence, the DietPositive markers showed a negative association, further indicating that taxa that respond positively to the diet negatively associate with those that are associated with frailty. (E) The negative association was further investigated by building networks for the five overlapping windows of samples W1–W5 (see Methods section), with increasing adherence to the diet. Relative co-occurrence propensity between the DietPositive and the module C across networks obtained for the overlapping windows of samples with increasing adherence to the diet. With increasing adherence to the diet, the relative co-occurrence propensity between the DietPositive OTUs and those belonging to the module C becomes increasingly negative. The p values of the significance of association are indicated as ****p<0.0001, ***p<0.001, **p<0.01, *p<0.05.

models to probe and identify the specific taxonomic signals that best predict increased adherence to the MedDiet.

We observed that increased adherence to the MedDiet modulates specific components of the gut microbiota that were associated with a reduction in risk of frailty, improved cognitive function and reduced inflammatory status. For reasons described above, these associations for some of the diet-modulated microbiome markers could only be observed at relatively weaker thresholds (rho <-0.09 and rho >0.07, FDR-corrected p values <0.2). This allowed for the visualisation and re-examination of the most predictive OTUs. However, the striking observation was the consistency of associations of the diet-modulated microbiome markers with biological markers of ageing (independent of nationality). The formulation and calculation of a single sample-specific microbiome index clarified these associations even further. For a single sample, this index provided a quantitative summary of the abundance patterns of the diet-responsive markers (the higher the value, the higher the abundance of DietPositive taxa and vice versa), thereby addressing the sample-specific variability associated with the individual markers. We showed that they were not only associated with dietary compliance but were consistently associated with frailty and inflammatory markers, thereby confirming their importance for health maintenance independent of other anthropometric confounders like age, body mass index and gender. In fact, the apparent lack of a direct link of the adherence score with frailty further hints that the response of an individual to the diet could be mediated by the change in the microbiome. Besides these associations, the keystone nature of the DietPositive markers within the gut microbiome remains remarkably stable across multiple nationalities. These keystone properties of the DietPositive markers add support to the so-called Anna Karenina principle[59] of microbiomes which posits that microbiomes of healthy individuals are similar and the unhealthy individuals are each aberrant in their own way. By protecting the 'core' of the gut microbial community, adherence to the diet could facilitate the retention of a stable community state in the microbiome, providing resilience and protecting from changes to alternative states that are found in unhealthy subjects.

The positive impact of these microbial taxa on host health was further indicated by predictive metabolite profiling, where

Gut: first published as 10.1136/gutjnl-2019-319654 on 17 February 2020. Downloaded from http://gut.bmj.com/ on February 17, 2023 by guest. Protected by copyright.

increasing adherence to the diet specifically selects for taxa that are enriched in the production of SCFAs/BCFAs, while selecting against those associated with bile acid dysregulation and production of proposed deleterious metabolites like acetone, p-cresol, ethanol and carbon dioxide. Although this is an in-silico prediction, an increase of SCFA production with MedDiet consumption (or with specific components of the MedDiet) has been previously shown.[10 50–52] The study by Pagliai *et al*, which compared the microbiome and metabolome changes on MedDiet and vegetarian diets, reported a significant positive association of carbohydrate consumption (which is increased in the MedDiet) with faecal levels of SCFA butyrate and a significant negative association of lipid and fat intake (decreased in the MedDiet) with levels of the SCFAs propionate and acetate. Negative associations of the SCFAs were also observed with levels of the inflammatory cytokine IL-17.[50] Although the study by Pagliai *et al* observed no significant differences in the levels of BCFAs on the MedDiet (in contrast to the in-silico predictive metabolite analysis performed in our current study), a negative association of the BCFA levels with fat intake was also observed (in line with our current findings). The links between the MedDiet-associated microbiome modulation, SCFA production and the carcinogenic secondary bile acid production are precisely in line with findings from two previous studies on African Americans and rural Africans.[51 52] Interestingly, across the secondary bile acid production landscape, while the faecal metabolome results from the study by O'Keefe *et al* confirmed the predicted metabolite changes with respect to CA and the carcinogenic secondary bile acids DCA and LCA, the plasma metabolite levels (in the current study) confirm the predicted changes with respect to CDCA and GCDCA (although plasma metabolite levels are not expected to exactly reflect the faecal metabolome). Thus, results obtained from these studies largely complement each other and resonate with our current findings, and the predicted downregulation of the other potentially detrimental metabolite production provides an informed list of candidate compounds that can be further verified by targeted metabolomic profiling in future studies.

The interplay of diet, microbiome and host health is a complex phenomenon influenced by several factors. It is also probably a multistep process dictated by specific mechanistic rules. While the results of this study shed light on some of the rules of this three-way interplay, several factors such as age, body mass index, disease status and initial dietary patterns may play a key role in determining the extent of success of these interactions. Interestingly, the beneficial effects of MedDiet intervention mediated through the microbiome are not restricted to elderly subjects, as evidenced by the study by Meslier *et al*[60] (this volume; co-submitted to *Gut* for back-to-back publication) showing that a similar intervention in obese subjects resulted in multiple health-related shifts in the gut microbiome and metabolome independently of energy intake. Notwithstanding this theoretical and practical reinforcement, the strategy of promoting health in the elderly by maintaining a long-term MedDiet (or supplementation of specific ingredients) may be impractically expensive or logistically impossible in many countries where these ingredients are neither staple nor available year-round. In some older subjects with problems like dentition, saliva production, dysphagia or irritable bowel syndrome, adapting a MedDiet may not be a realistic option. Our definition here of MedDiet-responsive taxa that correlate with health, plus our recent identification of taxa associated with healthy ageing in a large metacohort of 2500 subjects,[61] provides a short list of candidate taxa for development as live biotherapeutic agents for direct administration to older subjects to reduce onset of frailty.

Author affiliations
[1]School of Microbiology, University College Cork, Cork, Ireland
[2]APC Microbiome Ireland, University College Cork, Cork, Ireland
[3]Unit of Microbial Ecology of Health, Department of Pharmacy and Biotechnology, University of Bologna, Bologna, Italy
[4]Department of Experimental, Diagnostic and Speciality Medicine, Alma Mater Studiorum, University of Bologna, Bologna, Italy
[5]CIG Interdepartmental Centre "L Galvani", Alma Mater Studiorum, University of Bologna, Bologna, Italy
[6]Norwich Medical School, University of East Anglia Faculty of Medicine and Health Sciences, Norwich, Norfolk, UK
[7]Laboratory of Microbiology, Wageningen University and Research, Wageningen, Netherlands
[8]CRNH Auvergne, F-63000 Clermont-Ferrand, CHU Clermont-Ferrand, Clermont-Ferrand, France
[9]Unité de Nutrition Humaine, Université Clermont Auvergne, Clermont-Ferrand, Auvergne, France
[10]Plateforme d'Exploration du Métabolisme, MetaboHUB Clermont, Clermont-Ferrand, Université Clermont Auvergne, Clermont-Ferrand, Auvergne, France
[11]Division of Human Nutrition and Health, Wageningen University and Research, Wageningen, Netherlands
[12]Department of Human Nutrition, Warsaw University of Life Sciences, Warszawa, Poland
[13]Gut Health Institute Strategic Programme, Quadram Institute Bioscience, Norwich, UK
[14]Department of Experimental and Clinical Medicine, Section of Anatomy, University of Florence, Firenze, Toscana, Italy
[15]Human Microbiome Research Program, Faculty of Medicine, University of Helsinki, Helsinki, Finland
[16]Department of Nutrition and Preventive Medicine, Norwich Medical School, University of East Anglia, Norwich, UK
[17]The Institute of Global Food Security, Queen's University Belfast, Belfast, UK
[18]Unit of Microbial Ecology of Health, Department of Pharmacy and Biotechnology, University of Bologna, Bologna, Italy
[19]Department of Experimental, Diagnostic and Speciality Medicine, Alma Mater Studiorum, University of Bologna, Bologna, Emilia-Romagna, Italy
[20]Department of Applied Mathematics, Institute of Information Technology, Mathematics and Mechanics (ITMM), Lobachevsky State University of Nizhny Novgorod-National Research University (UNN), Nizhny Novgorod, Russian Federation

Contributors TSG, IBJ, POT, CF and AS conceived and designed the analysis. MN, AS, MC, EG, AJ, MC, ST, EGZ, GDAH, CE, NM, CMB, EP-G, AM, JK, BP, BC, MN, MM-F and others collected and/or contributed data. TSG, IBJ and SR performed the analysis. TSG, IBJ and POT wrote the paper assisted by SR, AS, PB, EGZ and WMDeV. WMDeV, SF-T, AC, PB, CF, POT and others reviewed the analysis and the manuscript.

Funding The authors are funded in part by Science Foundation Ireland (APC/SFI/12/RC/2273) in the form of a research centre, APC Microbiome Ireland. IBJ was supported by a Science Foundation Ireland grant (13/SIRG/2128). The NU-AGE project is supported by the European Union's Seventh Framework Programme under grant agreement no. 266 486 ('NU-AGE: New dietary strategies addressing the specific needs of the elderly population for healthy ageing in Europe').

Competing interests None declared.

Patient consent for publication Not required.

Provenance and peer review Not commissioned; externally peer reviewed.

Data availability statement Data are available upon reasonable request. The majority of results corresponding to the current study are included in the article or uploaded as supplementary information. Other data are available on request from the authors.

Open access This is an open access article distributed in accordance with the Creative Commons Attribution Non Commercial (CC BY-NC 4.0) license, which permits others to distribute, remix, adapt, build upon this work non-commercially, and license their derivative works on different terms, provided the original work is properly cited, appropriate credit is given, any changes made indicated, and the use is non-commercial. See: http://creativecommons.org/licenses/by-nc/4.0/.

ORCID iDs
Amy Jennings http://orcid.org/0000-0001-5333-714X
Gerben D A Hermes http://orcid.org/0000-0003-4314-9553
Joanna Kaluza http://orcid.org/0000-0001-9454-0929
Barbara Pietruszka http://orcid.org/0000-0003-0731-8612
Paul W O'Toole http://orcid.org/0000-0001-5377-0824

Gut: first published as 10.1136/gutjnl-2019-319654 on 17 February 2020. Downloaded from http://gut.bmj.com/ on February 17, 2023 by guest. Protected by copyright.

REFERENCES

1 Clegg A, Young J, Iliffe S, *et al*. Frailty in elderly people. *Lancet* 2013;381:752–62.
2 Cevenini E, Monti D, Franceschi C. Inflamm-ageing. *Curr Opin Clin Nutr Metab Care* 2013;16:14–20.
3 Franceschi C, Bonafè M, Valensin S, *et al*. Inflamm-aging. an evolutionary perspective on immunosenescence. *Ann N Y Acad Sci* 2000;908:244–54.
4 Sugimoto T, Sakurai T, Ono R, *et al*. Epidemiological and clinical significance of cognitive frailty: a mini review. *Ageing Res Rev* 2018;44:1–7.
5 Wilson D, Jackson T, Sapey E, *et al*. Frailty and sarcopenia: the potential role of an aged immune system. *Ageing Res Rev* 2017;36:1–10.
6 An R, Wilms E, Masclee AAM, *et al*. Age-dependent changes in GI physiology and microbiota: time to reconsider? *Gut* 2018;67:2213–22.
7 Trichopoulou A, Martínez-González MA, Tong TY, *et al*. Definitions and potential health benefits of the Mediterranean diet: views from experts around the world. *BMC Med* 2014;12:112.
8 Sofi F, Cesari F, Abbate R, *et al*. Adherence to Mediterranean diet and health status: meta-analysis. *BMJ* 2008;337:a1344.
9 Kojima G, Avgerinou C, Iliffe S, *et al*. Adherence to Mediterranean diet reduces incident frailty risk: systematic review and meta-analysis. *J Am Geriatr Soc* 2018;66:783–8.
10 De Filippis F, Pellegrini N, Vannini L, *et al*. High-Level adherence to a Mediterranean diet beneficially impacts the gut microbiota and associated metabolome. *Gut* 2016;65:1812–21.
11 Mitsou EK, Kakali A, Antonopoulou S, *et al*. Adherence to the Mediterranean diet is associated with the gut microbiota pattern and gastrointestinal characteristics in an adult population. *Br J Nutr* 2017;117:1645–55.
12 Claesson MJ, Jeffery IB, Conde S, *et al*. Gut microbiota composition correlates with diet and health in the elderly. *Nature* 2012;488:178–84.
13 O'Toole PW, Jeffery IB. *Gut microbiota and aging. (1095-9203 (Electronic))*.
14 Jeffery IB, Lynch DB, O'Toole PW. Composition and temporal stability of the gut microbiota in older persons. *ISME J* 2016;10:170–82.
15 Tran TTT, Cousin FJ, Lynch DB, *et al*. Prebiotic supplementation in frail older people affects specific gut microbiota taxa but not global diversity. *Microbiome* 2019;7:39.
16 Berendsen A, Santoro A, Pini E, *et al*. A parallel randomized trial on the effect of a healthful diet on inflammageing and its consequences in European elderly people: design of the NU-AGE dietary intervention study. *Mech Ageing Dev* 2013;134:523–30.
17 Marseglia A, Xu W, Fratiglioni L, *et al*. Effect of the NU-AGE diet on cognitive functioning in older adults: a randomized controlled trial. *Front Physiol* 2018;9:349.
18 Jennings A, Cashman KD, Gillings R, *et al*. A Mediterranean-like dietary pattern with vitamin D3 (10 µg/d) supplements reduced the rate of bone loss in older Europeans with osteoporosis at baseline: results of a 1-y randomized controlled trial. *Am J Clin Nutr* 2018;108:633–40.
19 Maijo M, Ivory K, Clements SJ, *et al*. One-year consumption of a Mediterranean-like dietary pattern with vitamin D3 supplements induced small scale but extensive changes of immune cell phenotype, co-receptor expression and innate immune responses in healthy elderly subjects: results from the United Kingdom arm of the NU-AGE trial. *Front Physiol* 2018;9:997.
20 Jennings A, Berendsen AM, de Groot LCPGM, *et al*. Mediterranean-style diet improves systolic blood pressure and arterial stiffness in older adults. *Hypertension* 2019;73:578–86.
21 Santoro A, Pini E, Scurti M, *et al*. Combating inflammaging through a Mediterranean whole diet approach: the NU-AGE project's conceptual framework and design. *Mech Ageing Dev* 2014;136-137:3–13.
22 Santoro A, Guidarelli G, Ostan R, *et al*. Gender-specific association of body composition with inflammatory and adipose-related markers in healthy elderly Europeans from the NU-AGE study. *Eur Radiol* 2019;29:4968–79.
23 Yu Z, Morrison M. Improved extraction of PCR-quality community DNA from digesta and fecal samples. *Biotechniques* 2004;36:808–12.
24 Costea PI, Zeller G, Sunagawa S, *et al*. Towards standards for human fecal sample processing in metagenomic studies. *Nat Biotechnol* 2017;35:1069–76.
25 Magoč T, Salzberg SL. FLASH: fast length adjustment of short reads to improve genome assemblies. *Bioinformatics* 2011;27:2957–63.
26 Edgar RC. Search and clustering orders of magnitude faster than BLAST. *Bioinformatics* 2010;26:2460–1.
27 Edgar RC, Haas BJ, Clemente JC, *et al*. UCHIME improves sensitivity and speed of chimera detection. *Bioinformatics* 2011;27:2194–200.
28 Allard G, Ryan FJ, Jeffery IB, *et al*. SPINGO: a rapid species-classifier for microbial amplicon sequences. *BMC Bioinformatics* 2015;16:324.
29 Wang Q, Garrity GM, Tiedje JM, *et al*. Naive Bayesian classifier for rapid assignment of rRNA sequences into the new bacterial taxonomy. *Appl Environ Microbiol* 2007;73:5261–7.
30 Faust K, Sathirapongsasuti JF, Izard J, *et al*. Microbial co-occurrence relationships in the human microbiome. *PLoS Comput Biol* 2012;8:e1002606.
31 Gusenleitner D, Howe EA, Bentink S, *et al*. iBBiG: iterative binary bi-clustering of gene sets. *Bioinformatics* 2012;28:2484–92.
32 Noronha A, Modamio J, Jarosz Y, *et al*. The virtual metabolic human database: integrating human and gut microbiome metabolism with nutrition and disease. *Nucleic Acids Res* 2019;47(D1):D614–24.
33 Sung J, Kim S, Cabatbat JJT, *et al*. Global metabolic interaction network of the human gut microbiota for context-specific community-scale analysis. *Nat Commun* 2017;8:15393.
34 Shannon P, Markiel A, Ozier O, *et al*. Cytoscape: a software environment for integrated models of biomolecular interaction networks. *Genome Res* 2003;13:2498–504.
35 Berendsen AAM, van de Rest O, Feskens EJM, *et al*. Changes in dietary intake and adherence to the NU-AGE diet following a one-year dietary intervention among European older adults: results of the NU-AGE randomized trial. *Nutrients* 2018;10:E1905.
36 Machiels K, Joossens M, Sabino J, *et al*. A decrease of the butyrate-producing species Roseburia hominis and Faecalibacterium prausnitzii defines dysbiosis in patients with ulcerative colitis. *Gut* 2014;63:1275–83.
37 Qin J, Li Y, Cai Z, *et al*. A metagenome-wide association study of gut microbiota in type 2 diabetes. *Nature* 2012;490:55–60.
38 Yu J, Feng Q, Wong SH, *et al*. Metagenomic analysis of faecal microbiome as a tool towards targeted non-invasive biomarkers for colorectal cancer. *Gut* 2017;66:70–8.
39 Jackson MA, Jackson M, Jeffery IB, *et al*. Signatures of early frailty in the gut microbiota. *Genome Med* 2016;8:8.
40 Gomez-Arango LF, Barrett HL, Wilkinson SA, *et al*. Low dietary fiber intake increases Collinsella abundance in the gut microbiota of overweight and obese pregnant women. *Gut Microbes* 2018;9:189–201.
41 Kovatcheva-Datchary P, Shoaie S, Lee S, *et al*. Simplified intestinal microbiota to study microbe-diet-host interactions in a mouse model. *Cell Rep* 2019;26:3772–83.
42 Qin N, Yang F, Li A, *et al*. Alterations of the human gut microbiome in liver cirrhosis. *Nature* 2014;513:59–64.
43 Karlsson FH, Fåk F, Nookaew I, *et al*. Symptomatic atherosclerosis is associated with an altered gut metagenome. *Nat Commun* 2012;3:1245.
44 Giampieri E, Ostan R, Guidarelli G, *et al*. A novel approach to improve the estimation of a diet adherence considering seasonality and short term variability - the NU-AGE Mediterranean diet experience. *Front Physiol* 2019;10:149.
45 Ouchi N, Walsh K. Adiponectin as an anti-inflammatory factor. *Clin Chim Acta* 2007;380:24–30.
46 Jones SA, Scheller J, Rose-John S. Therapeutic strategies for the clinical blockade of IL-6/gp130 signaling. *J Clin Invest* 2011;121:3375–83.
47 Chávez-Talavera O, Tailleux A, Lefebvre P, *et al*. Bile acid control of metabolism and inflammation in obesity, type 2 diabetes, dyslipidemia, and nonalcoholic fatty liver disease. *Gastroenterology* 2017;152:1679–94.
48 Tsuei J, Chau T, Mills D, *et al*. Bile acid dysregulation, gut dysbiosis, and gastrointestinal cancer. *Exp Biol Med* 2014;239:1489–504.
49 Sanna S, van Zuydam NR, Mahajan A, *et al*. Causal relationships among the gut microbiome, short-chain fatty acids and metabolic diseases. *Nat Genet* 2019;51:600–5.
50 Pagliai G, Russo E, Niccolai E, *et al*. Influence of a 3-month low-calorie Mediterranean diet compared to the vegetarian diet on human gut microbiota and SCFA: the CARDIVEG study. *Eur J Nutr* 2019;11.
51 Ou J, Carbonero F, Zoetendal EG, *et al*. Diet, microbiota, and microbial metabolites in colon cancer risk in rural Africans and African Americans. *Am J Clin Nutr* 2013;98:111–20.
52 O'Keefe SJD, Li JV, Lahti L, *et al*. Fat, fibre and cancer risk in African Americans and rural Africans. *Nat Commun* 2015;6:6342.
53 Bone E, Tamm A, Hill M. The production of urinary phenols by gut bacteria and their possible role in the causation of large bowel cancer. *Am J Clin Nutr* 1976;29:1448–54.
54 Elshaghabee FMF, Bockelmann W, Meske D, *et al*. Ethanol production by selected intestinal microorganisms and lactic acid bacteria growing under different nutritional conditions. *Front Microbiol* 2016;7:47.
55 Baskaran S, Rajan DP, Balasubramanian KA. Formation of methylglyoxal by bacteria isolated from human faeces. *J Med Microbiol* 1989;28:211–5.
56 Khan MT, Nieuwdorp M, Bäckhed F. Microbial modulation of insulin sensitivity. *Cell Metab* 2014;20:753–60.
57 Ghoshal UC, Shukla R, Ghoshal U. Small intestinal bacterial overgrowth and irritable bowel syndrome: a bridge between functional organic dichotomy. *Gut Liver* 2017;11:196–208.
58 Durack J, Lynch SV. The gut microbiome: relationships with disease and opportunities for therapy. *J Exp Med* 2019;216:20–40.
59 Zaneveld JR, McMinds R, Vega Thurber R. Stress and stability: applying the Anna Karenina principle to animal microbiomes. *Nat Microbiol* 2017;2:17121.
60 Ercolini D, De Filippis F, Roager HM. Mediterranean diet intervention in overweight and obese subjects lowers plasma cholesterol and causes changes in the gut microbiome and metabolome independently of energy intake. *Gut* 2020;69:1258–68.
61 Ghosh D, Jeffery O' Toole. Adjusting for age improvesidentification of gut microbiome alterations in multiple diseases. *eLife* In Press.

Gut: first published as 10.1136/gutjnl-2019-319654 on 17 February 2020. Downloaded from http://gut.bmj.com/ on February 17, 2023 by guest. Protected by copyright.

Supplementary Table 1: Numbers and demographics of subjects in control and intervention cohorts

	Controls						MedDiet Intervention					
	All Countries	Italy	UK	Netherlands	Poland	France	All Countries	Italy	UK	Netherlands	Poland	France
Individuals with sequenced microbiome	289	91	16	37	105	40	324	112	32	38	112	39
Median Age (Min-Max)	71 (65-79)	72 (65-79)	70.5 (65-79)	71.5 (65-79)	72 (65-79)	68 (65-77)	71 (65-79)	72 (65-79)	70.5 (65-79)	71.5 (65-79)	72 (65-79)	68 (65-72)
Gender (Male:Female)	145:144	46:45	7:9	21:16	46:59	25:15	141:182	56:56	12:20	13:25	45:67	15:24
Median BMI (Min-Max)	26.8 (18.8-44.6)	26.4 (18.8-44.6)	27.20 (20-31.5)	26.7 (19.7-35.1)	26.4 (21-37.6)	25.05 (18.9 – 37.5)	26.9 (18.5-46)	27.15 (18.7-37.9)	25.95 (18.5-33.7)	25 (20.3-35.8)	28.1 (19.5-46)	24.3 (19.7-31.3)

*: Baseline

SUPPLEMENTARY TEXT 1

MEASUREMENT OF INFLAMMATORY AND ADIPOSITY RELATED HORMONES

Briefly, fresh blood from each participant was collected after fasting in each recruiting centre. Blood was immediately centrifuged at 2000 x g for 10 min at 4°C and separated into plasma and serum according to a standardized operating procedure. All the specimens were stored at -80 until the time of analysis and sent to the project partners responsible for the analyses. A magnetic bead-based multiplex immunoassay (Bio-Plex) (BIO-RAD laboratories, Milan, Italy) was used to measure the inflammatory and adiposity related markers according to the manufacturer's instructions. In particular, Interleukin (IL) 1beta, 1Ra, 2, 4, 5, 6, 7, 8 10, 12p70, 13, 17, 17A, 18, Tumor Necrosis Factor alpha (TNFα), Interferon gamma (INFγ), Granulocyte Macrophage Colony-Stimulating Factor (GM-CSF), Granulocyte Colony-Stimulating Factor (G-CSF), Macrophage inflammatory protein-1beta (MIP1β) and Monocyte Chemotactic Protein-1 (MCP-1), were measured in multiplex with Bio-Plex Pro Cytokine, Chemokine, and Growth Factor Assays (intra-assay coefficient of variation (CV) was lower than 4.55% for all the molecules); Transforming Growth Factor beta1 (TGF-β1 intra-assay CV, 3.83%) with Bioplex Pro TGF- beta assay; Ghrelin (inter-assay CV, 2%) and Resistin (inter-assay CV, 4%) in multiplex with Bio-Plex Pro human diabetes assay. Plates were read and analyzed by Bio-Plex Manager Software. The level of Interleukin 6 receptor alpha (IL6rα, inter-assay CV, 3.1%)), Glycoprotein 130 (gp130, inter-assay CV, 5.9%), Pentraxin-3 (inter-assay CV, 6.8%) and soluble TNFalpha receptors R1 (TNF-R1, inter-assay CV, 6.1%) and R2 (TNF-R2, inter-assay CV, 7.7%) were assessed in multiplex in a subgroup of 360 samples with Bioplex Pro human inflammation assay (gp-130, inter-assay %CV 5.9). The quantitative determination of hsCRP, leptin, adiponectin has been performed by ProcartaPlexTM Immunoassay (eBioscience, Hatfield, UK) according to the manufacturer's instructions. Analysis was performed using Luminex 200 instrumentation (Luminex Corportation, The Netherlands). Assay sensitivities were 19.31 pg/mL for Leptin, 4.39 pg/mL for hsCRP, and 47.46 pg/mL for adiponectin.

SUPPLEMENTARY TEXT 2

METHODOLOGY OF DNA EXTRACTION AND GENERATION OF 16S rRNA AMPLICON READS

A 250 mg stool sample was incubated with 1 ml lysis buffer (500 mM NaCl, 50 mM tris-HCl, pH 8.0, 50 mM EDTA and 4% sodium dodecyl sulphate (SDS)) in a 2-ml screw cap tube with 0.5 g sterile 0.1 mm zirconia beads and four sterile 3.5 mm glass beads (BioSpec Products, Bartlesville, OK). This was homogenised three times for 60 s at maximum speed (Mini-Beadbeater™, BioSpec Products), with cooling on ice for 60 s between homogenisation cycles. Samples were incubated at 95 °C for 15 min to further lyse the cells. Samples were centrifuged (16,000g) at 4 °C for 5 min and the supernatant was collected. For increased yield, an additional 300 µl of RBB lysis buffer was added to the pellet and the RBB steps were repeated as before. The supernatants were pooled and incubated with 350 µl of 7.5 M ammonium acetate (Sigma Aldrich, …) for 10 min. The protein-free DNA was precipitated with isopropanol at 4 °C and centrifuged at 16,000g. The pellet was washed with 70% (v/v) ethanol, allowed to dry, re-suspended in TE buffer, and treated with 10 mg/ml RNAse A (Thermo Scientific, Ireland). Proteinase K treatment and remaining DNA isolation was performed on-column using the QIAamp DNA Stool Mini Kit (Qiagen, Hilden, Germany) according to manufacturers' instructions leading to 200 µl of DNA eluted in AE buffer. DNA was visualised on a 0.8% agarose gel for quality assessment and quantified using a NanoDrop 2000 system (Thermo Scientific). DNA was stored at −20 °C until use.

16S rRNA gene libraries for the Illumina MiSeq System were prepared manually following the manufacturer's protocol (15031942; Illumina, San Diego, CA, USA), with some modifications. V3 and V4 region of 16S rRNA genes were amplified using 15 ng of DNA template, Phusion HF Master Mix (Thermo Scientific) and 0.2 µM primers (98 °C 30 s; 25 cycles of 98 °C 10 s, 55 °C 15 s, 72 °C 20 s; 72 °C 5 min)(60). Amplicons were cleaned up using SPRIselect magnetic beads (Beckman Coulter, Indianapolis, IN) and checked for quality on a 1.2% agarose gel. Cleaned amplicons (5 µl) were used as template for Index PCR using Phusion HF Master Mix and Nextera XT Index Kit v2 Set A and D (Illumina) (98 °C 30 s; 8 cycles of 98 °C 30 s, 55 °C 30 s, 72 °C 30 s; 72 °C 5 min). Indexed amplicons were cleaned up using SPRIselect magnetic beads, run on a 1.2% agarose gel and quantified by Qubit dsDNA HS Assay (Thermo Scientific). The samples were pooled in equimolar amounts (40 ng DNA per sample) with up to 288 samples per library. Final library sizes were validated using Bioanalyzer DNA 1000 chips (Agilent Technologies, Santa Clara, CA). Libraries were denatured with 0.2 N NaOH

and diluted to 6 pmol/L with a 20% PhiX control before loading onto the MiSeq flow cell. Sequencing was performed on an Illumina MiSeq platform using a 2 × 250 bp paired end protocol, as per manufacturer's instructions (Illumina), on multiple sequencing runs.

SUPPLEMENTARY FIGURES

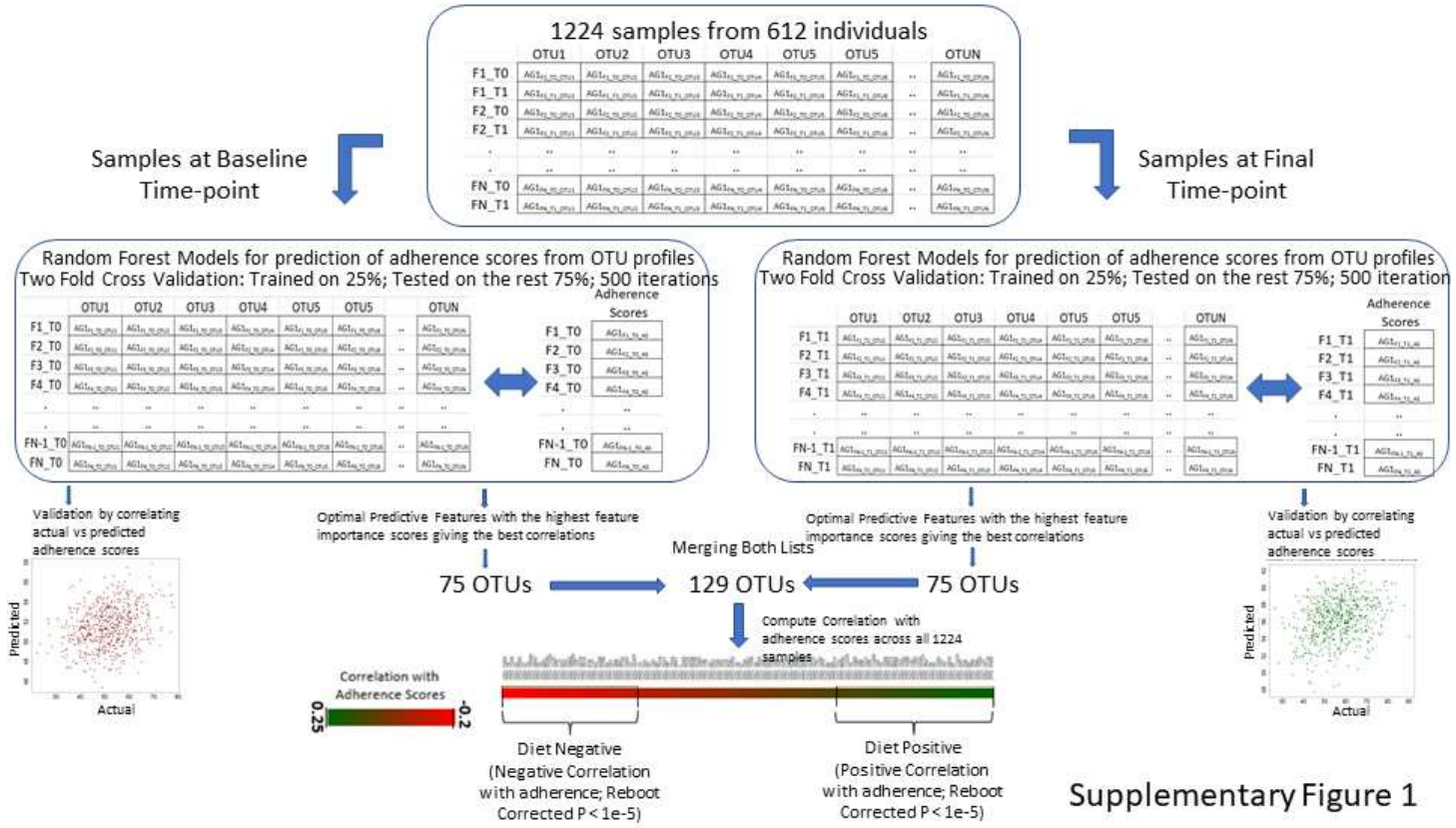

Supplementary Figure 1: Pictorial workflow describing the Random Forest based prediction of adherence scores from the microbiome abundance profiles and the identification of adherence score associated markers including the DietPositive and DietNegative markers.

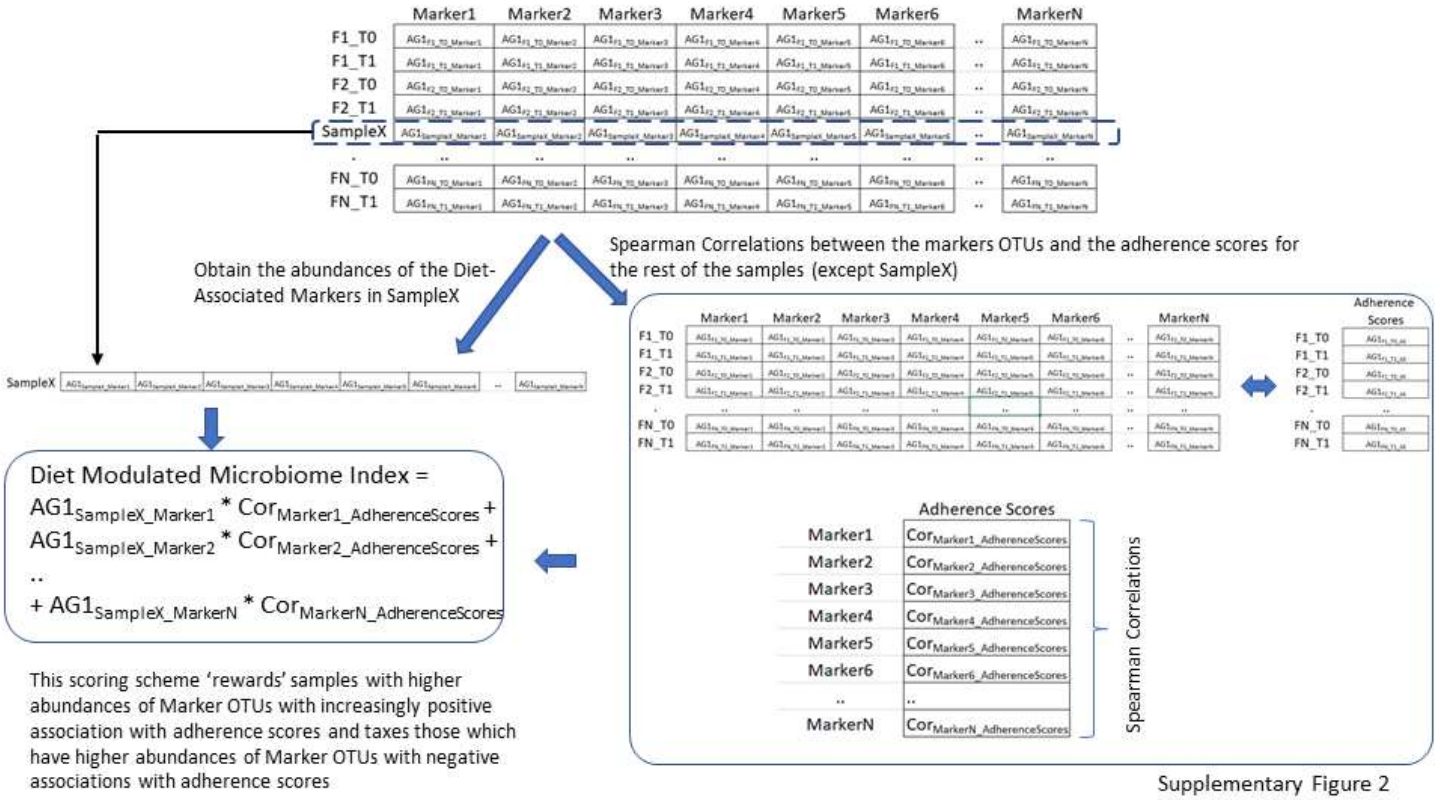

Supplementary Figure 2: Pictorial representation of the methodology of computation of the microbiome indices using the leave-one-out strategy.

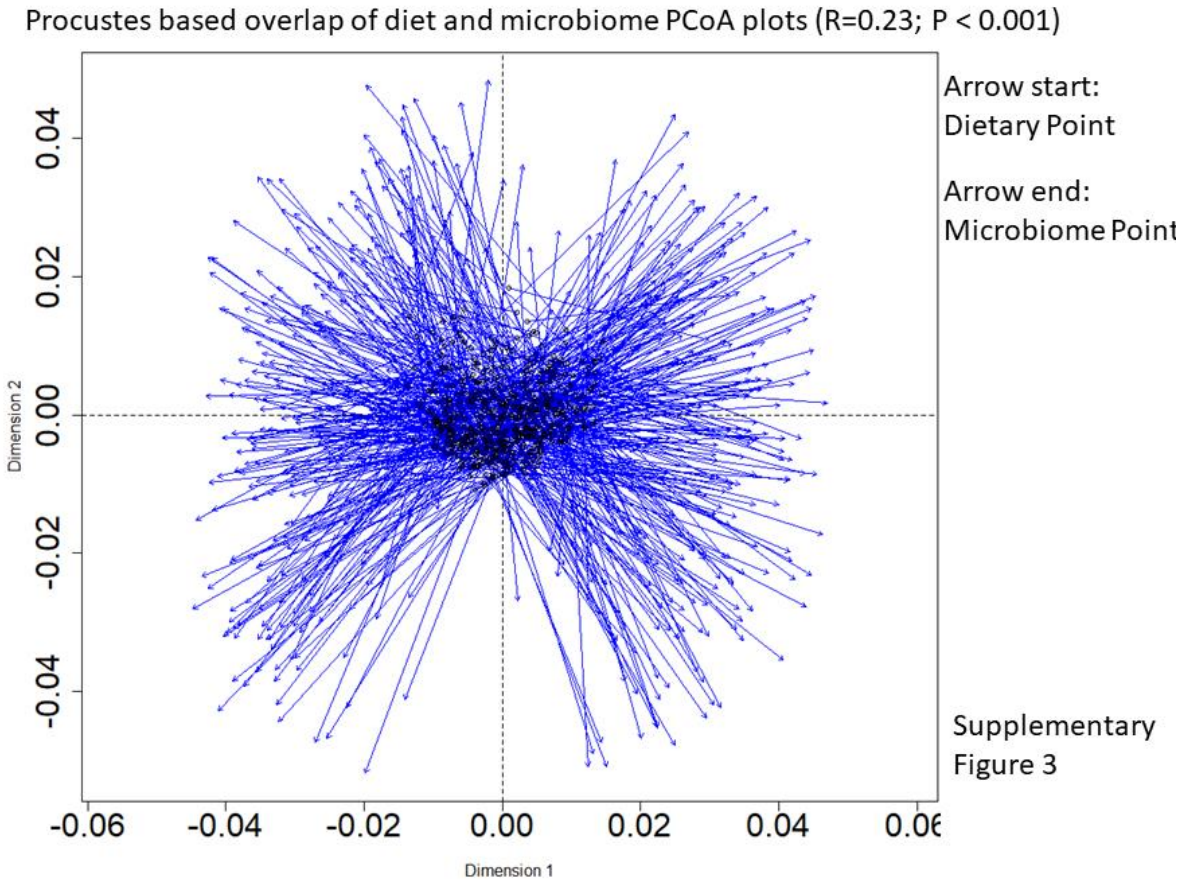

Supplementary Figure 3: Procustes plot showing the relative movement of the samples between the Principal Coordinate Analysis (PCoA) plots of the dietary and the microbiome profiles.

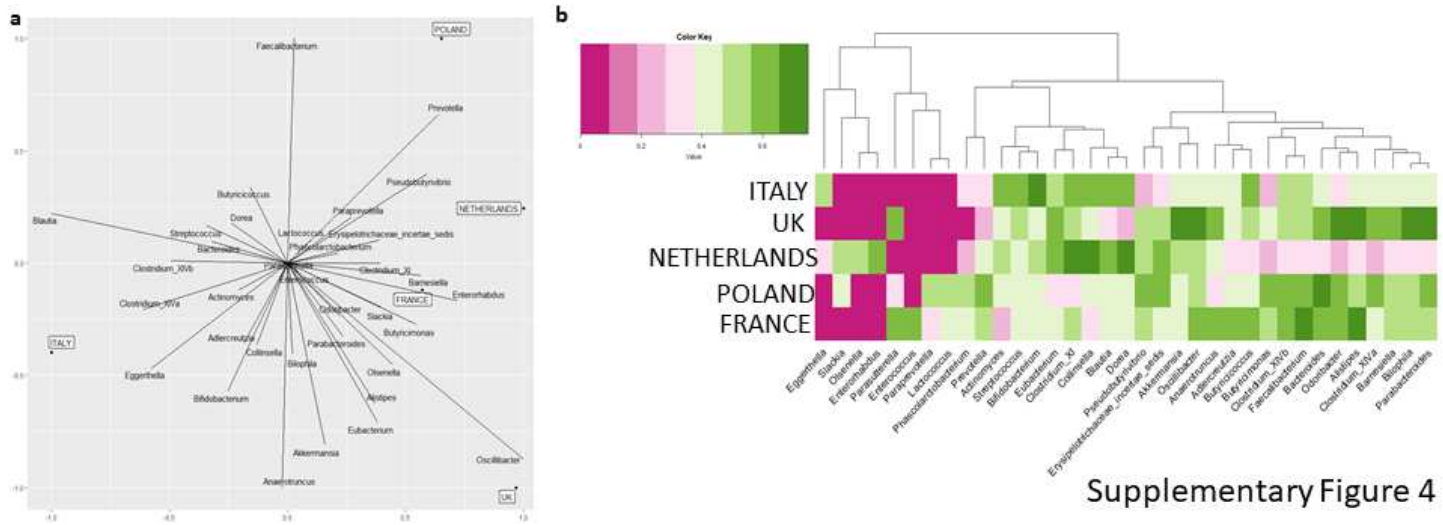

Supplementary Figure 4: Association of different genera with the specific nationalities shown as **a.** Plotted based on the weights of their association with the Principal Coordinate Analysis (PCoA) axes (as in Fig 1b). **b.** Plotted as heatmap showing the nationality-specific median abundances. Only those genera that are significantly over-abundant in at least one nationality as compared to the rest (Mann-Whitney tests using FDR corrected p-value < 0.15). Principal Component Analysis plots showing the changes in the microbiome profiles of subjects belonging to the various nationalities in **c.** control **d.** intervention cohorts. The p-values (obtained using envfit) of the association between the country and change of the microbiome in both the control and intervention cohorts are also indicated.

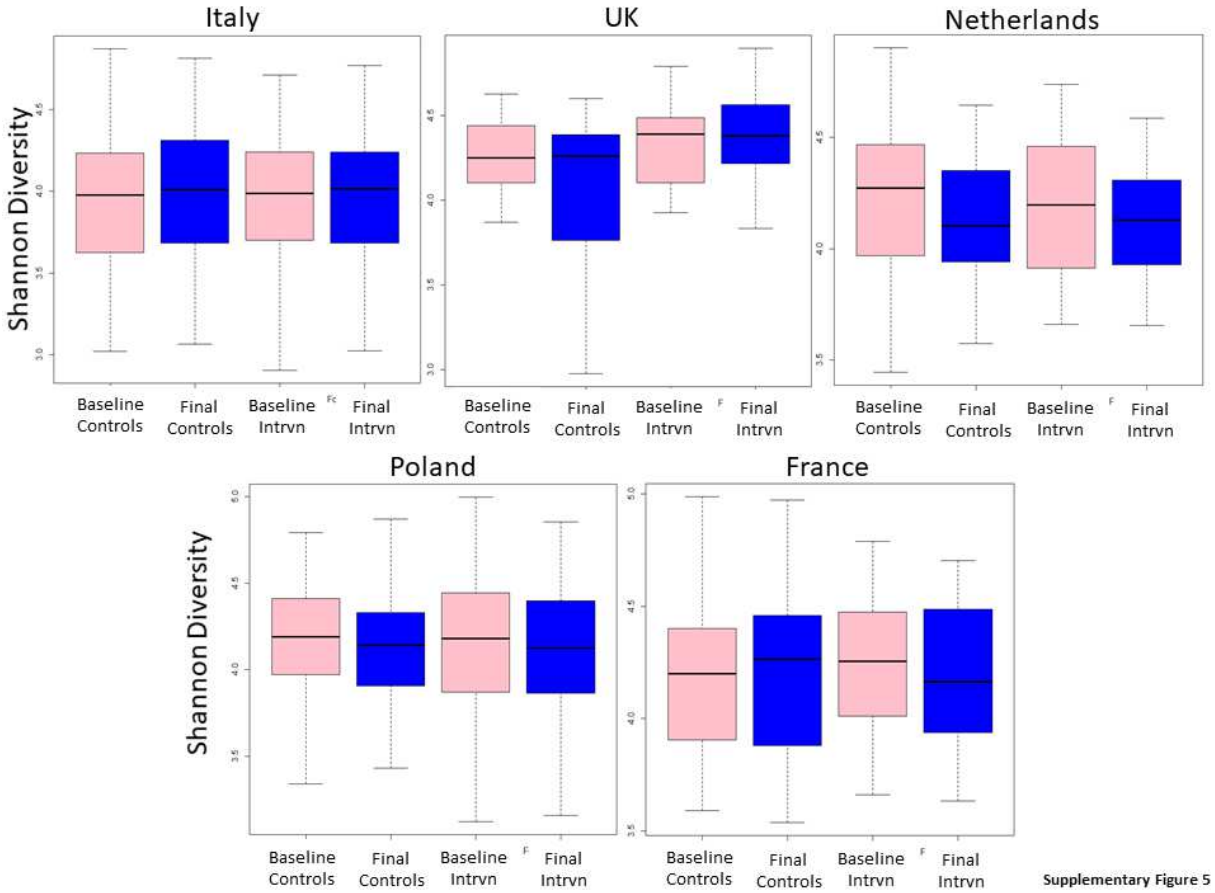

Supplementary Figure 5: Shannon diversity indices of the microbiota at baseline and Final time points for subjects in the intervention and control cohorts in the five different countries.

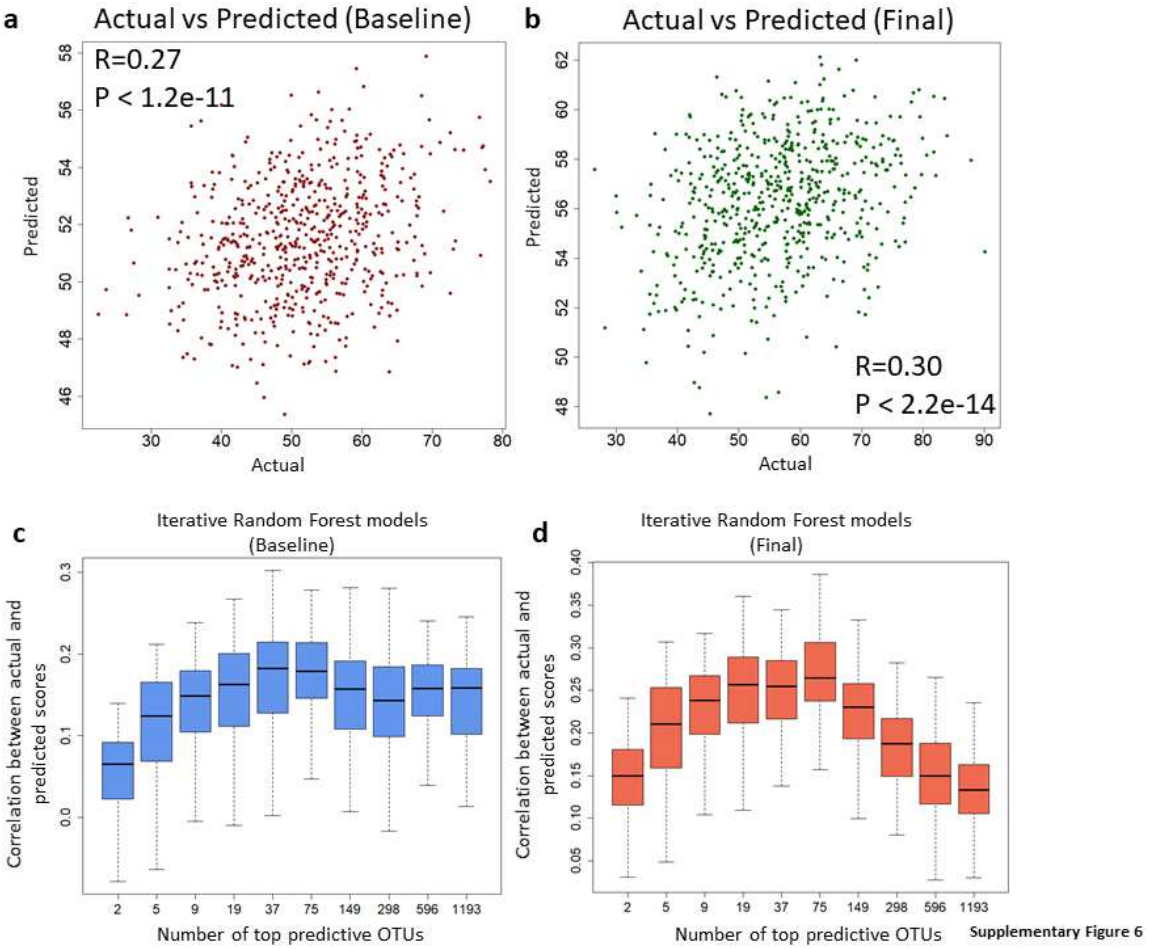

Supplementary Figure 6: Relationship between the Random Forest predicted and the actual dietary adherence scores for **a.** Baseline and **b.** Final time points. Boxplots showing the variation of the correlations between the actual and predicted dietary adherence scores obtained using iterative Random Forest prediction models with different number of top predictive features for **c.** Baseline and **d.** Final time-points. For both the time-points, the performance was observed to peak when the number of top features used was 75. Based on this, threshold of 75 top features was obtained for both time-points. The merger of the two lists of 75 features produced the final list of 129 features having optimal predictive ability across at least one of the time points.

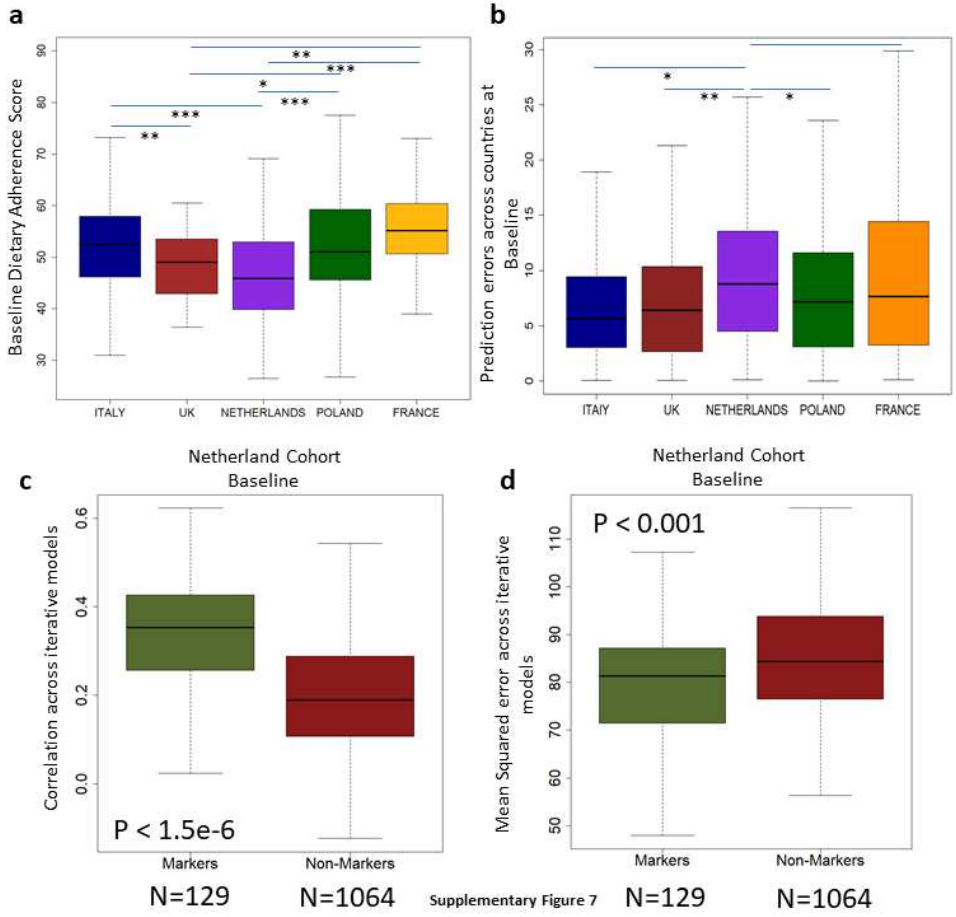

Supplementary Figure 7: a. Baseline Dietary Adherence Scores for the five different nationalities. **b.** Mean squared dietary adherence prediction errors for samples from five different nationalities **c.** Correlations and **d.** Mean squared errors between actual and predicted dietary adherence scores obtained using two different versions of iterative Random Forest models (two fold cross validation) separately for the samples from Netherlands (at baseline), While the first version was built using the set of 129 Diet-Associated Marker taxa as described in the previous figures (labelled as 'Markers') and the other using all 1064 OTUs besides the Diet-Associated Markers (labelled as 'Non-Markers').

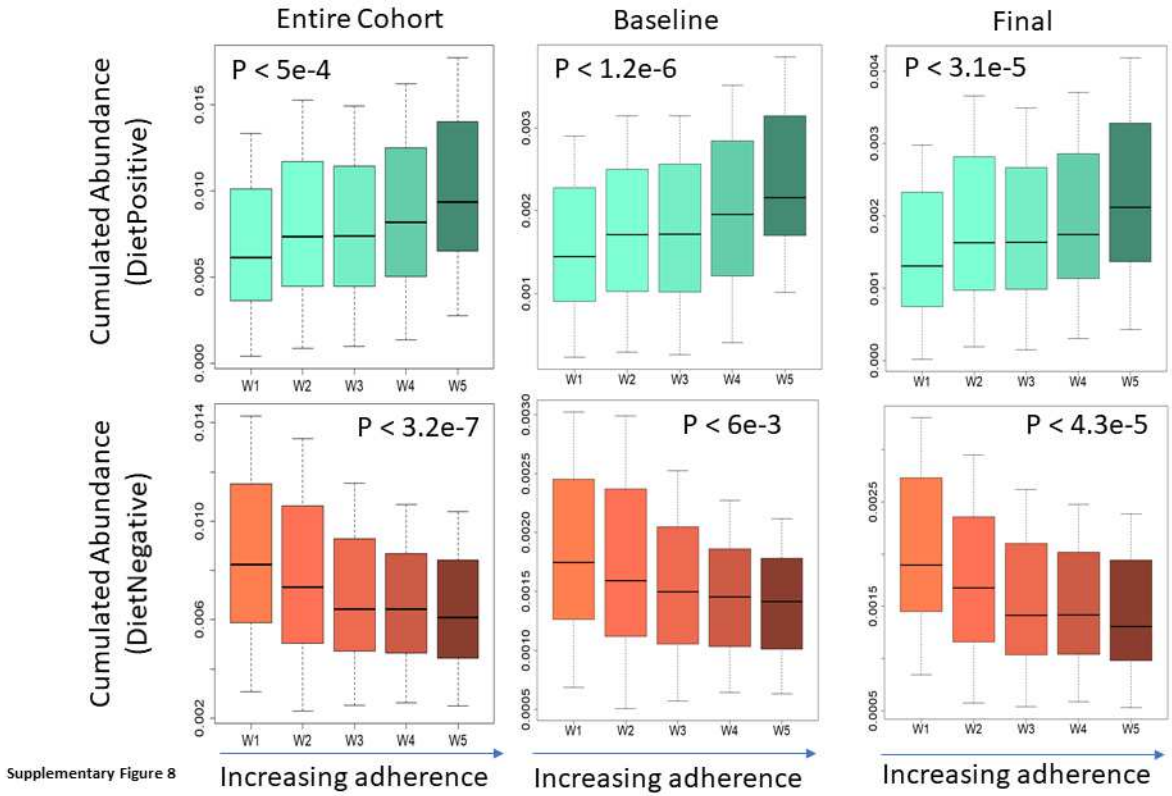

Supplementary Figure 8: Boxplots showing the variation of the cumulated abundances of the DietPositive and the DietNegative OTUs across overlapping windows of subjects with increasing adherence to the diet across the entire cohort as well as within the samples for the baseline and post-intervention time points (**See Methods**).

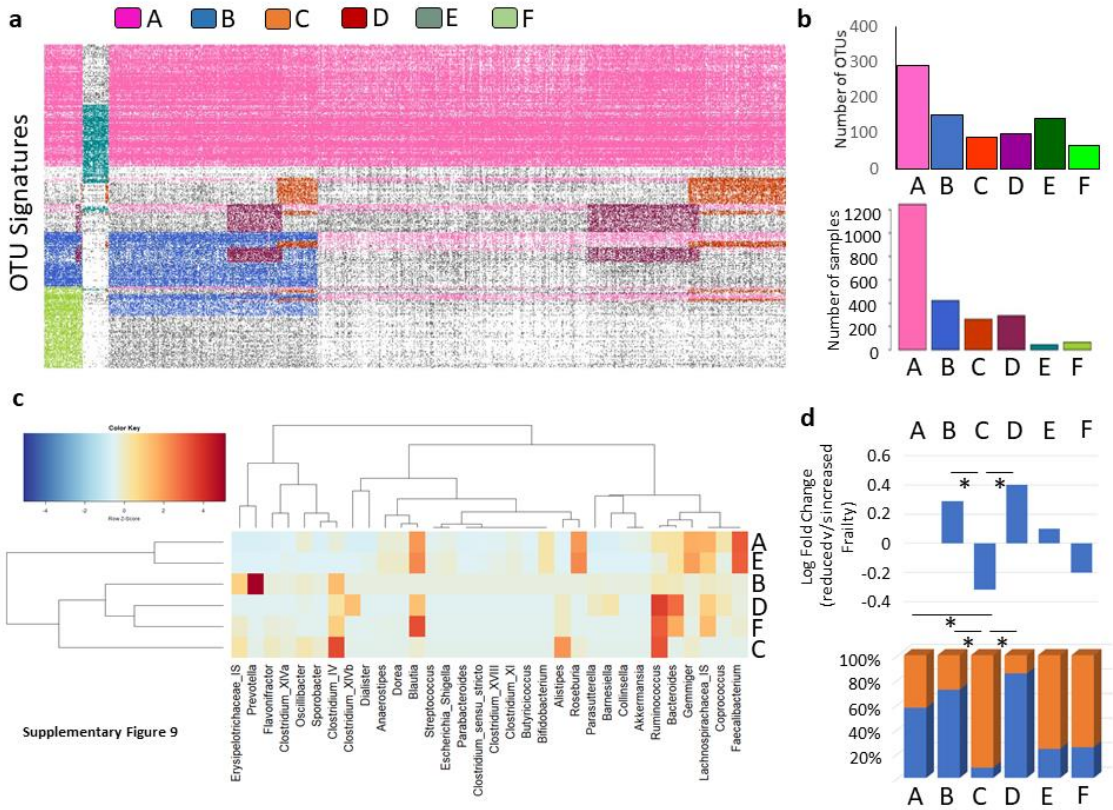

Supplementary Figure 9. Detection of specific taxonomic modules across the gut microbiomes using the iBBiG approach and association of specific modules with dietary adherence and reduced frailty. a. OTU detection profiles of the various modules obtained using the iBBiG approach. The color codes used for the various modules are: the primary core 'A' in pink; the Prevotella-associated 'B' in blue; the Alistipes-associated 'C' in orange; the Bacteroides-associated 'D' in maroon; the reduced core 'E' in darkgreen and; 'F' in light green. b. Bar-plot showing the number of samples containing each module (top) as well as the number of OTUs constituting each module (bottom). c. Heatmap showing the normalized abundances of the various genera within the OTUs constituting each module. d. Relative association of each of the modules with diet scores and frailty. The proportion bar-plots on the top right show the relative representation of the OTUs showing positive and negative association with diet scores within each module. The bar-plot on the bottom shows the log-fold increase in the number of samples containing each module in the individuals with reduced frailty (across time-points) as compared to those showing no change or an increase of frailty. Overall, these trends show the specific association of certain iBBiG modules with diet and frailty. While Modules B and D are associated positively with the Mediterranean diet and reduced frailty, Modules C shows the opposite trend.

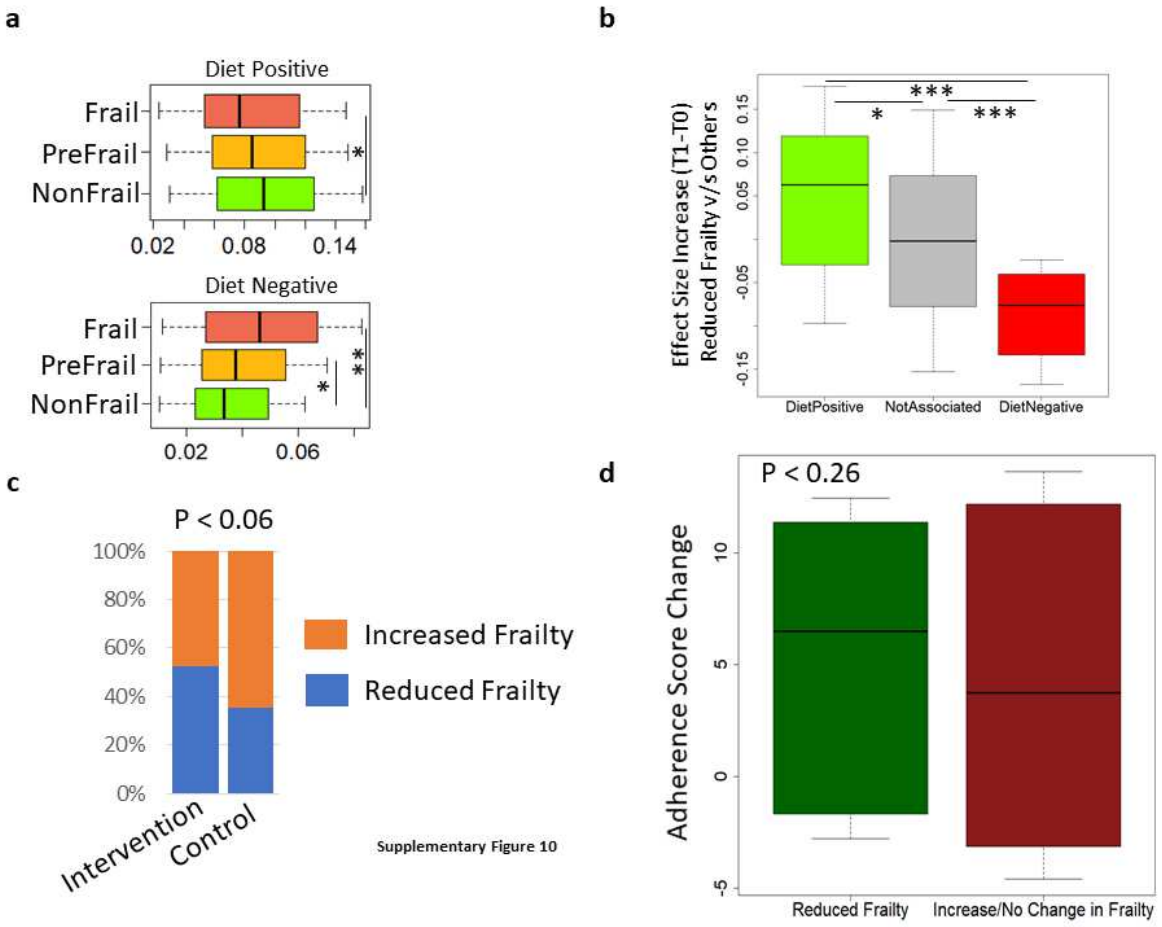

Supplementary Figure 10: **a.** Boxplots showing the variation of the cumulated abundance of the DietPositive and DietNegative OTUs in the Frail, Pre-Frail and the Non-Frail individuals. **b.** Variation of the effect-size differences (cohens' d) of the across time-point changes of the DietPositive OTUs, DietNegative OTUs and Not-Associated OTUs in Individuals with Reduced Frailty versus those with Increased or No Change in Frailty. **c.** Proportional representation of individuals with reduced and increased frailty in the control and intervention cohort. There was a marginally significant increase (Fishers' test P-value) in the representation of individuals with increased frailty in the control cohort. d. Boxplots showing the variation of adherence score changes in individuals with reduced frailty and those with increased or no change in frailty status.

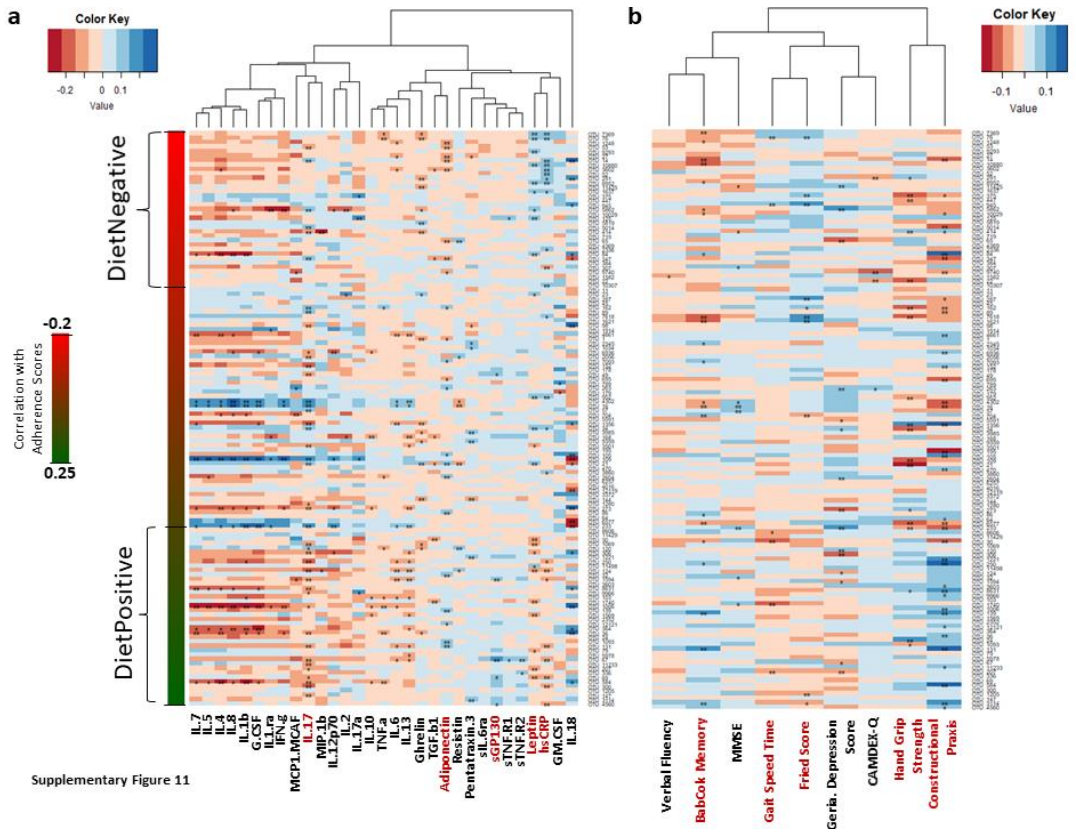

Supplementary Figure 11

Supplementary Figure 11: Heatmap showing the variation of the association patterns (obtained using Spearman Rhos) of the adherence associated marker OTUs (arranged from top to bottom in increasing order of their correlations with the adherence scores) with a. each of the pro/anti-inflammatory cytokine levels and b. the different measures of frailty, cognitive function. For each cell, colors indicate the Spearman Rho values (as shown), ** indicates a significant association with FDR corrected P-value < 0.15, * indicates a marginal association with nominal P-value < 0.05. The DietPositive and the DietNegative OTUs are also demarcated. Measures highlighted in red are those, for which the association patterns with the individual OTUs were observed to exhibit significant positive or negative correlations (Spearman correlation FDR corrected P-value < 0.15) with the OTU-adherence score association values.

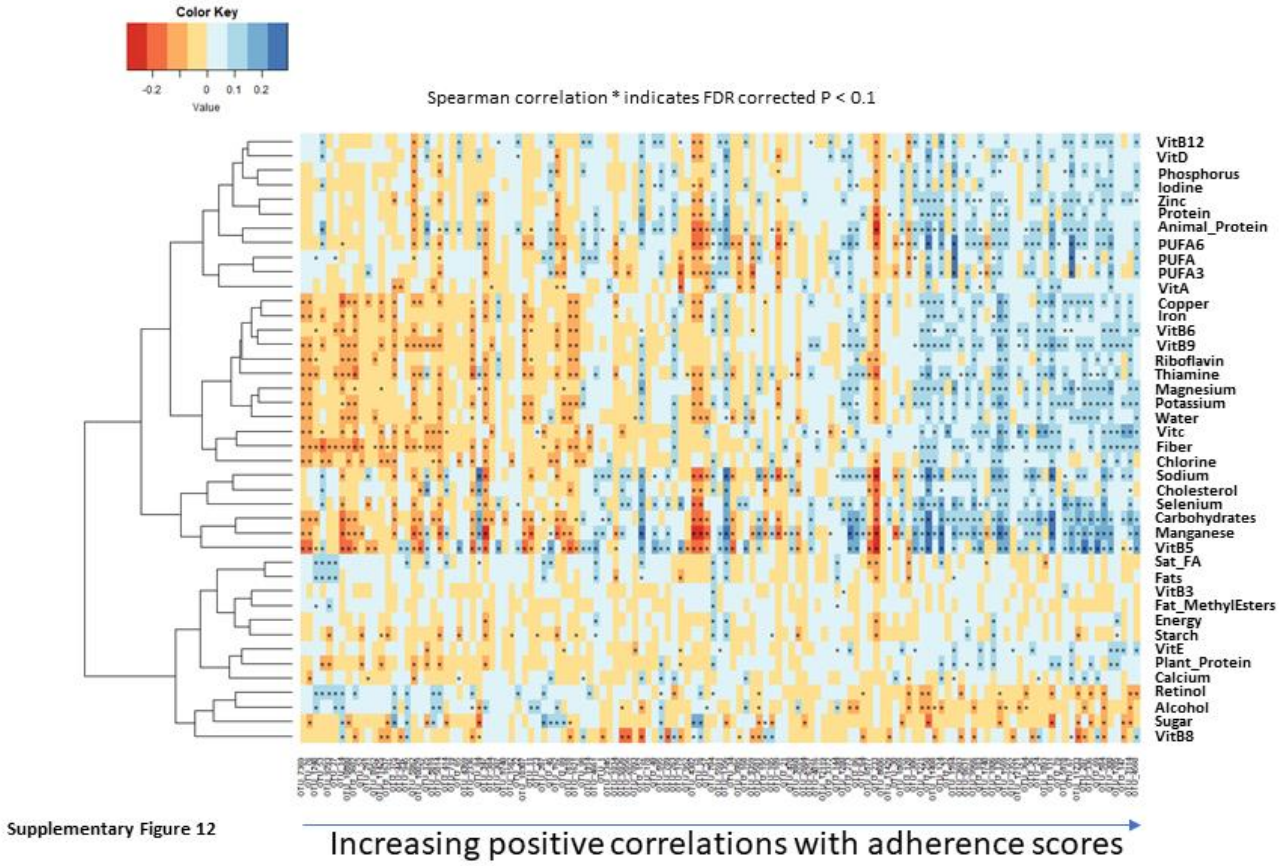

Supplementary Figure 12: Heatmap showing the partial spearman associations of the different dietary components with the marker OTUs arranged in increasing order of their association with the dietary adherence scores. For each marker OTU, partial spearman correlations were obtained after adjusting for the confounding effects of age, BMI, gender, country and poly-pharmacy.

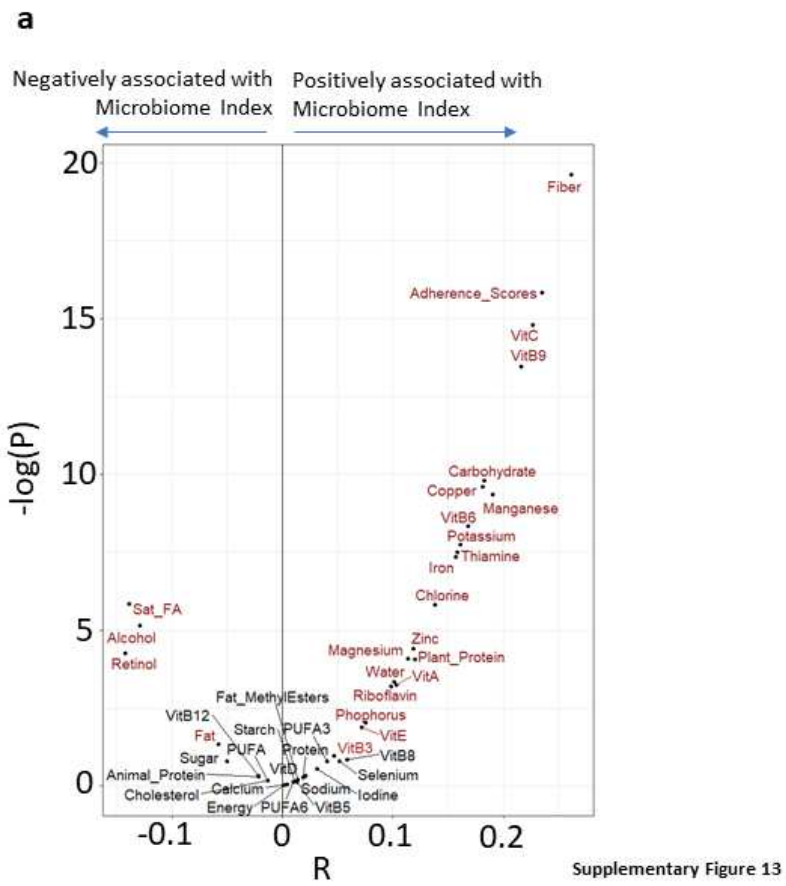

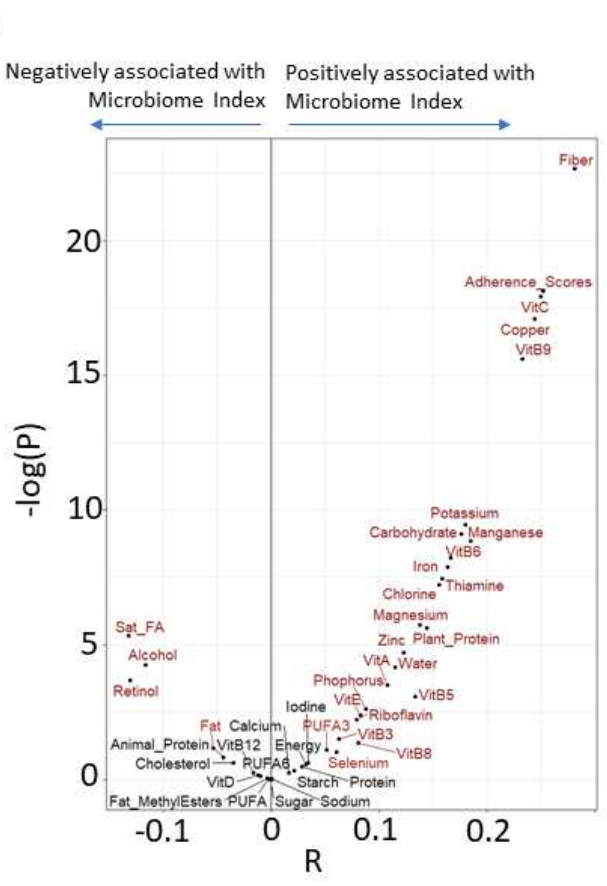

Supplementary Figure 13

Supplementary Figure 13. Violin plots showing the a. Partial spearman correlations between the consumption of different dietary components and the microbiome index across all time-points taking into account age, bmi, gender, country and poly-pharmacy. b. Partial spearman correlations between the consumption of different dietary components and the microbiome index across all subjects at the baseline taking into account age, bmi, gender, country, disease-status and poly-pharmacy.

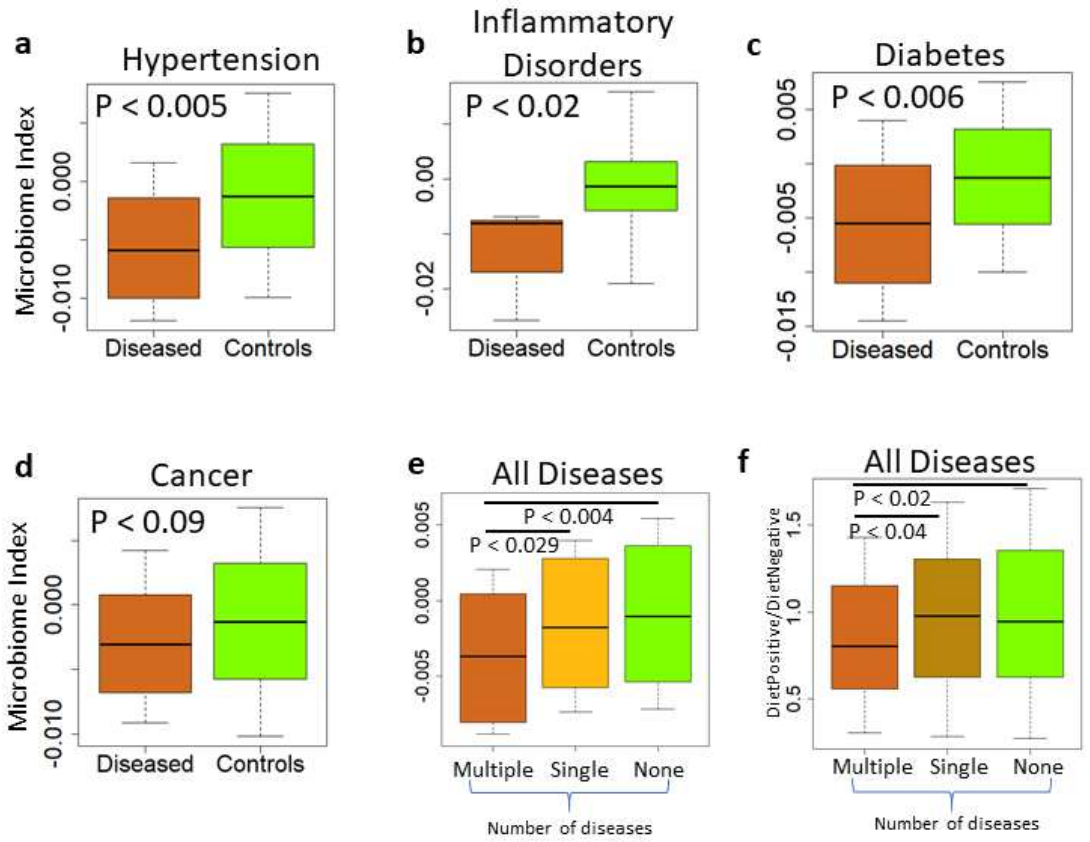

Supplementary Figure 14

Supplementary Figure 14. Boxplot showing the comparison of the MedDiet modulated microbiome index for individuals suffering from heart attack (**a**), inflammatory disorders (**b**), Type II Diabetes (**c**) and Cancer (**d**) with the control individuals (tagged as no-disease) at baseline. Boxplot showing the variation of microbiome index (**e**) and the abundance ratio of the DietPositive to DietNegative markers (**f**) for individuals with multiple, single and no-diseases at the baseline. The P-values of the Mann-Whitney U tests are also indicated for each pairwise-comparisons.

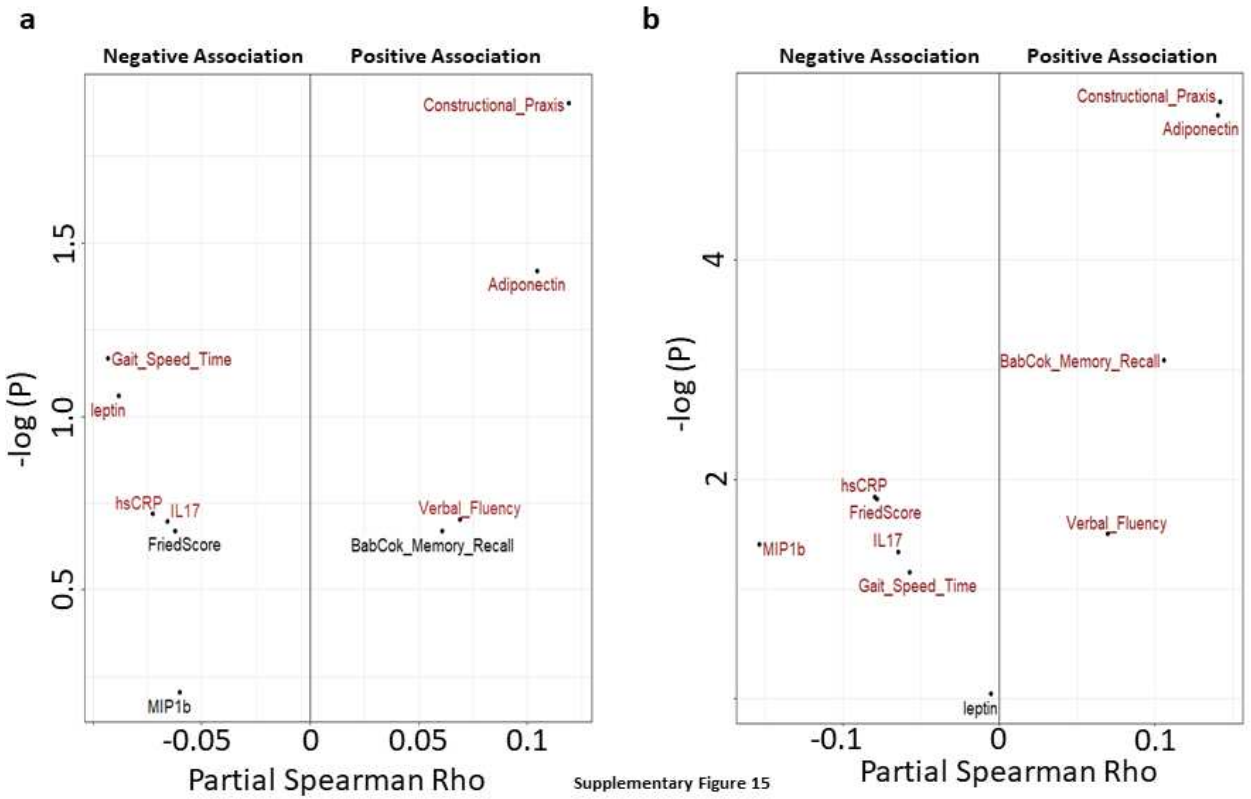

Supplementary Figure 15

Supplementary Figure 15: a. Violin plot showing the association (partial Spearman correlations) of the different measures of frailty, cognitive function and inflammatory marker levels (identified in figure 4) with the MedDiet modulated Microbiome index at the baseline after taking into account the age, BMI, gender, nine different disease pathologies (with greater or equal to 10 subjects), polypharmacy and gender as a confounder. b. Violin plot showing the association (partial Spearman correlations) of the different measures of frailty, cognitive function and inflammatory marker levels (identified in figure 4) with the MedDiet modulated Microbiome index at both the baseline and follow-up time points after taking into account the age, BMI, gender, polypharmacy and gender as a confounder. X-axis contains the spearman Rho values, and Y-axis indicates the -log (base 10) of the P-values. While most negatively associated measures are expected to be extreme left of the plot, the most positively associated measures are expected to be extreme right of the plot. Points are colored based on the significance of the obtained associations (Red indicates associations with FDR corrected P-value < 0.1).

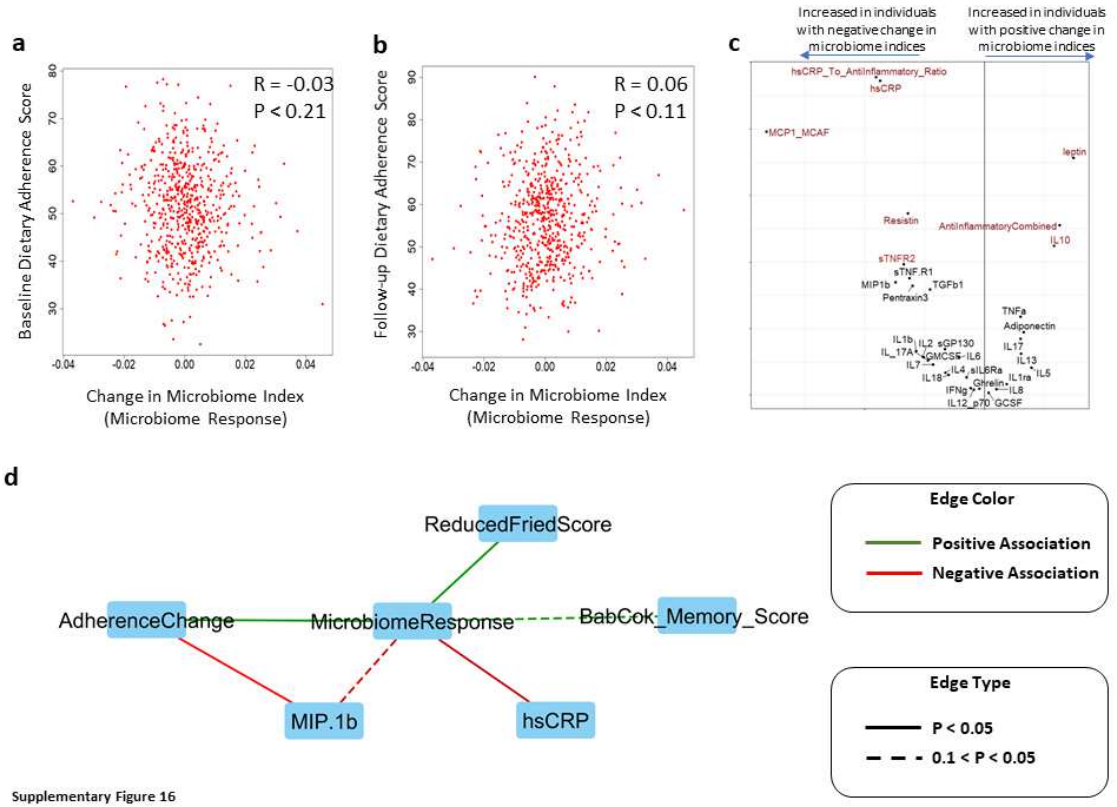

Supplementary Figure 16: Scatterplots showing the correlation between the microbiome response (that is the across time-point change in microbiome indices) and a. Baseline dietary adherence scores and b. final dietary adherence scores. c. Violin plots showing the spearman correlations of the changes in the different cytokine levels with the change in microbiome indices between the follow-up and baseline time points. X-axis contains the spearman Rho values, and Y-axis indicates the -log (base 10) of the P-values. While most negatively associated measures (that is those cytokines for which negative changes in levels are associated with positive changes in microbiome indices) are expected to be extreme left of the plot, the most positively associated measures (that is those cytokines for which positive changes in levels are associated with positive changes in microbiome indices) are expected to be extreme right of the plot. Points are colored based on the significance of the obtained associations (Red indicates associations with FDR corrected P-value < 0.1). Cumulated levels of anti-inflammatory cytokines were calculated as the mean ranked abundances of anti-inflammatory cytokines IL-10, IL-4, IL-5 and IL-1ra. Ratios of hsCRP to anti-inflammatory cytokines were calculated as ratios of the ranked abundance of hsCRP and the mean ranked abundances of anti-inflammatory cytokines IL-10, IL-4, IL-5 and IL-1ra. d. Graph showing the marginal or significant associations (dotted line indicating marginal associations with P < 0.1 and solid line indicating P < 0.05) between the across time-point changes of the various measures obtained using pairwise linear regressions.

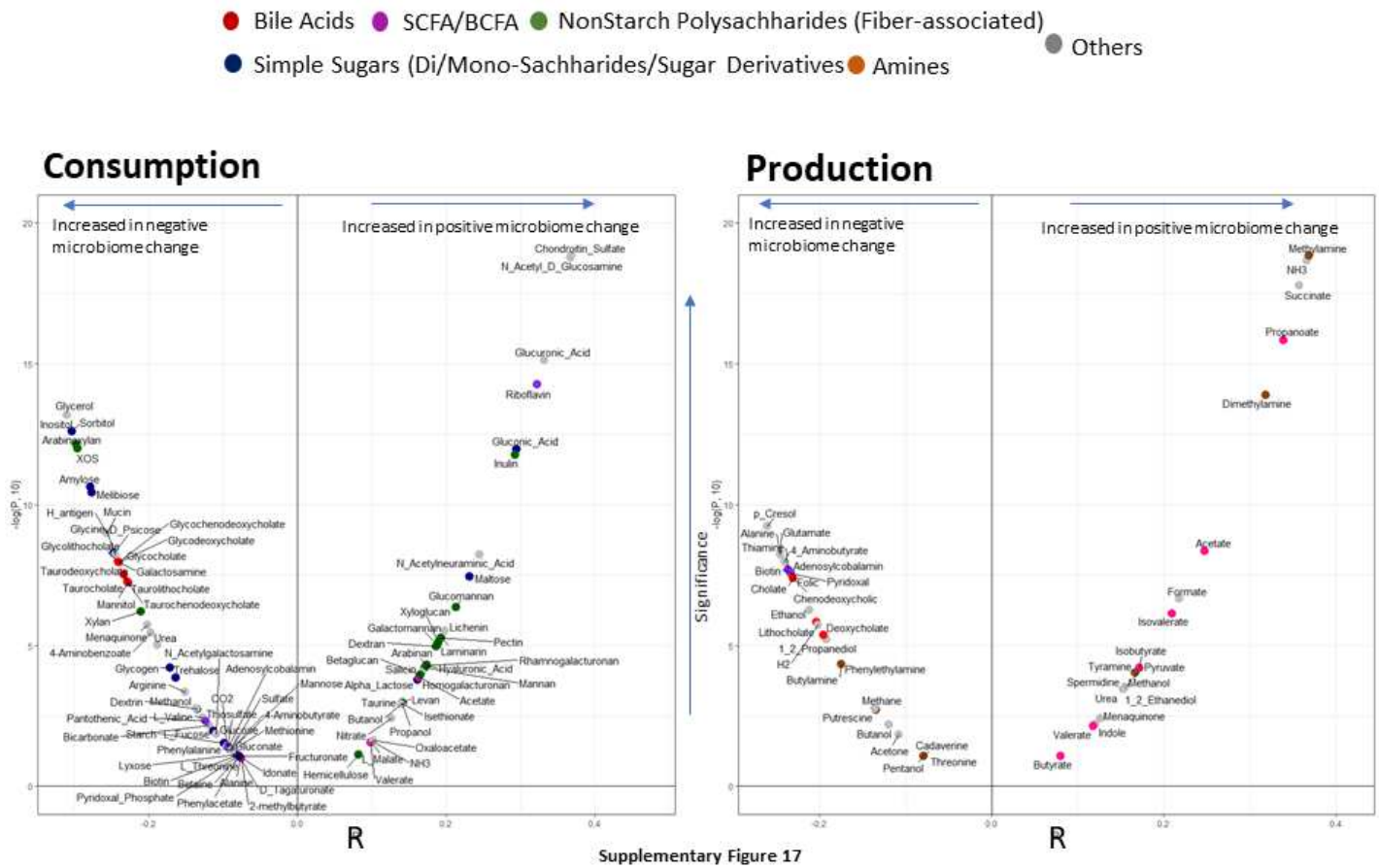

Supplementary Figure 17: Violin plots showing the inferred metabolite **a.** consumption and **b.** production profiles showing significant (positive or negative) associations (Spearman correlation; FDR corrected P-value < 0.15) with microbiome responses. While most negatively associated measures are expected to be extreme left of the plot, the most positively associated measures are expected to be extreme right of the plot. The points are colored based on the metabolite groups as indicated on the top panel of the Figure.

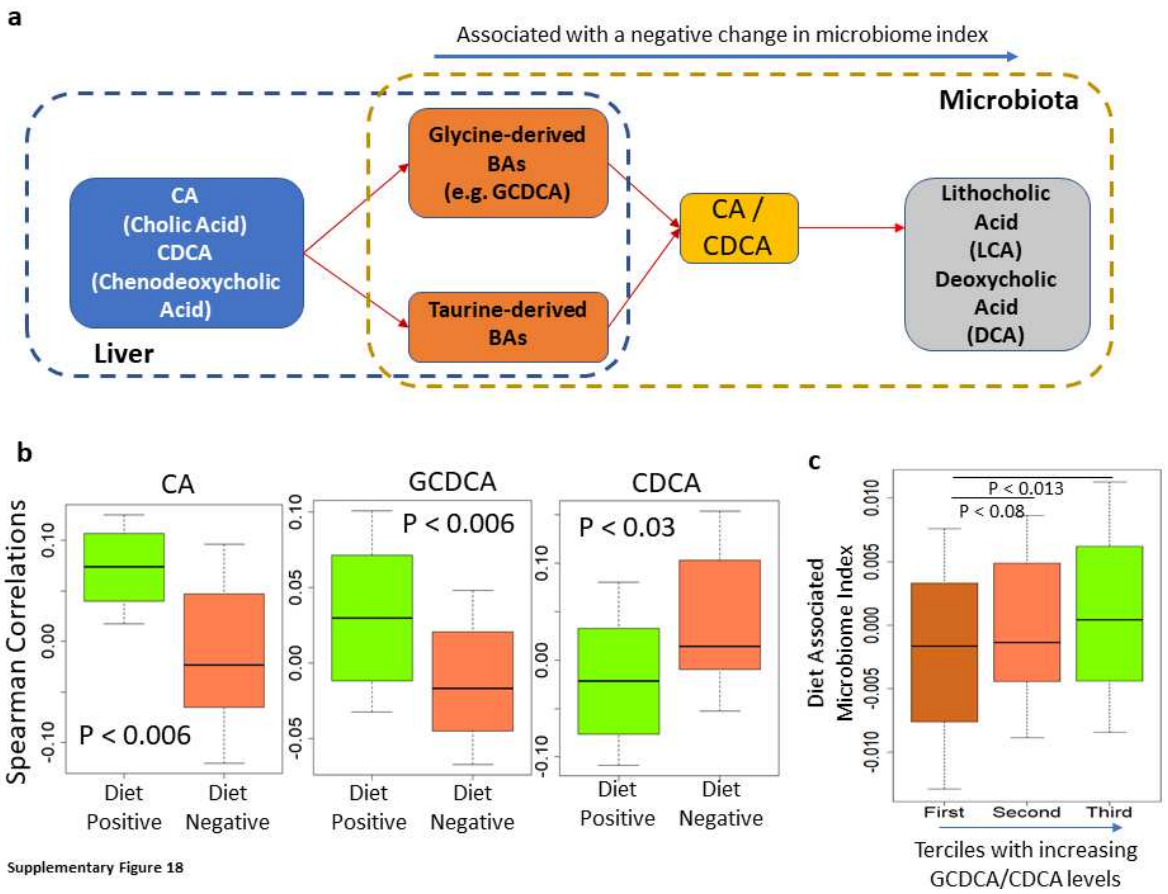

Supplementary Figure 18. a. Schematic representation of the bile acid conversion pathway, highlighting the specific sub-module converting glycine/taurine-conjugated bile acids (like TCA, GCDCA) to carcinogenic secondary bile acids (LCA/DCA), through CA and CDCA, that is associated with a negative change in microbiome index highlighted in red. b. Boxplots showing the spearman correlations of the abundances of the DietPositive and DietNegative OTUs with the measured plasma levels of CA, DCA and GCDCA for the subset of Italian and Polish individuals. c. Boxplot comparing the across the time-point changes in the microbiome index for individuals with increasing GCDCA/CA levels (grouped into three equal terciles with increasing GCDCA/CA ratios). P-values of pairwise Mann-Whitney U-tests are also indicated.

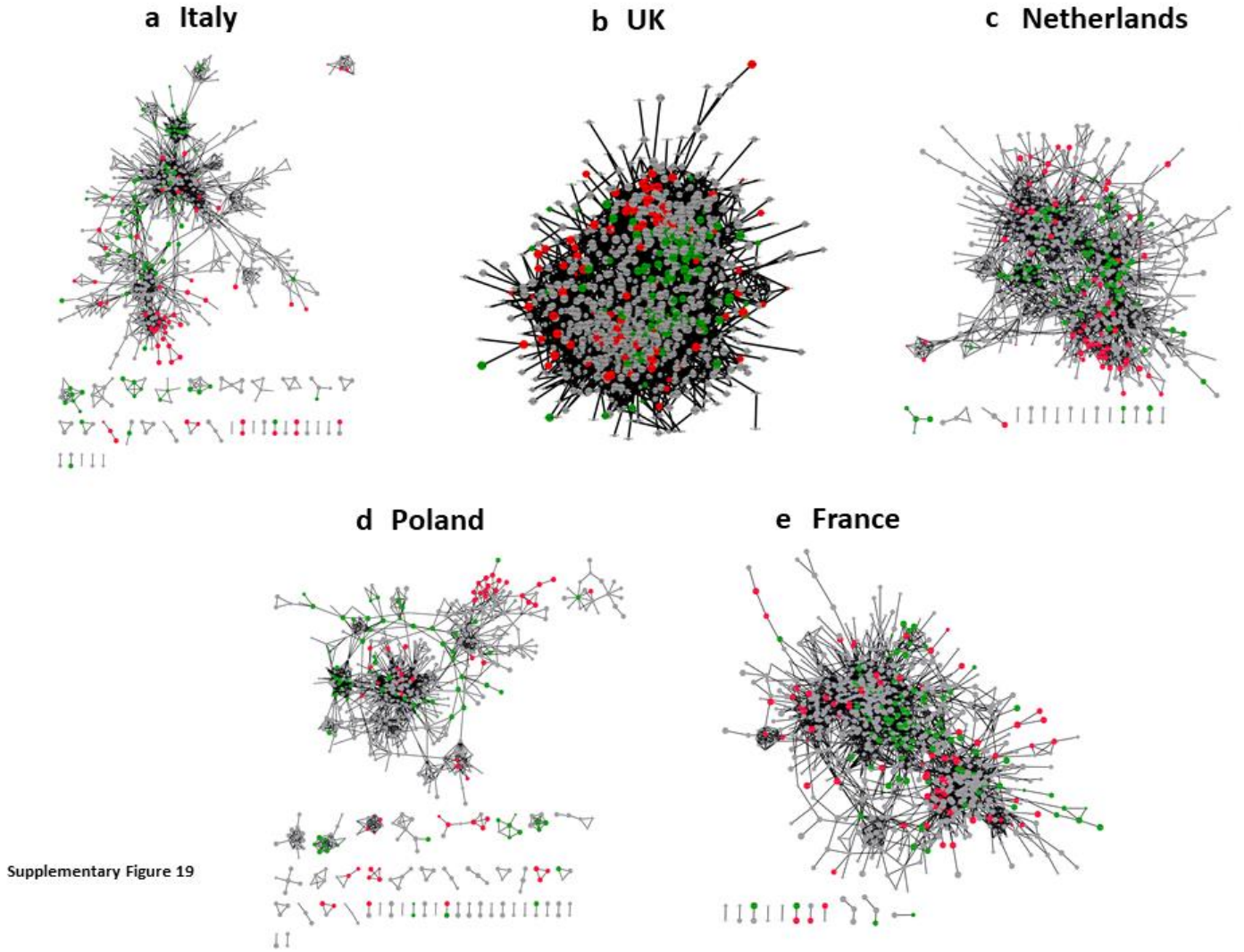

Supplementary Figure 19: Inter-OTU co-occurrence networks obtained for the different nationalities. DietPositive, DietNegative and the non-associated OTUs are shown in green, red and gray color, respectively. Despite variations in their overall structures, all networks gave a clear picture whereby in the DietPositive taxa were placed in the centre of the neworks, while the DietNegative taxa in the periphery.

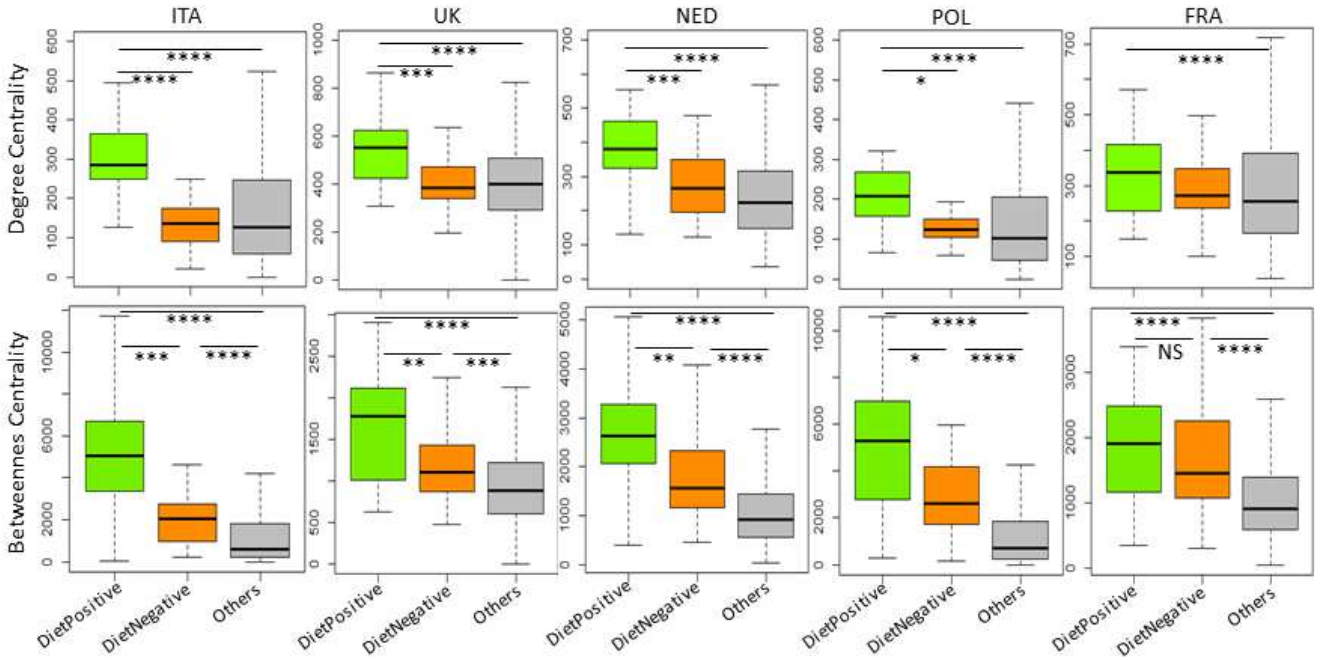

Supplementary Figure 20

Supplementary Figure 20: Variation of the degree and betweenness centrality of the different groups of taxa within the co-occurrence networks for the different nationalities.

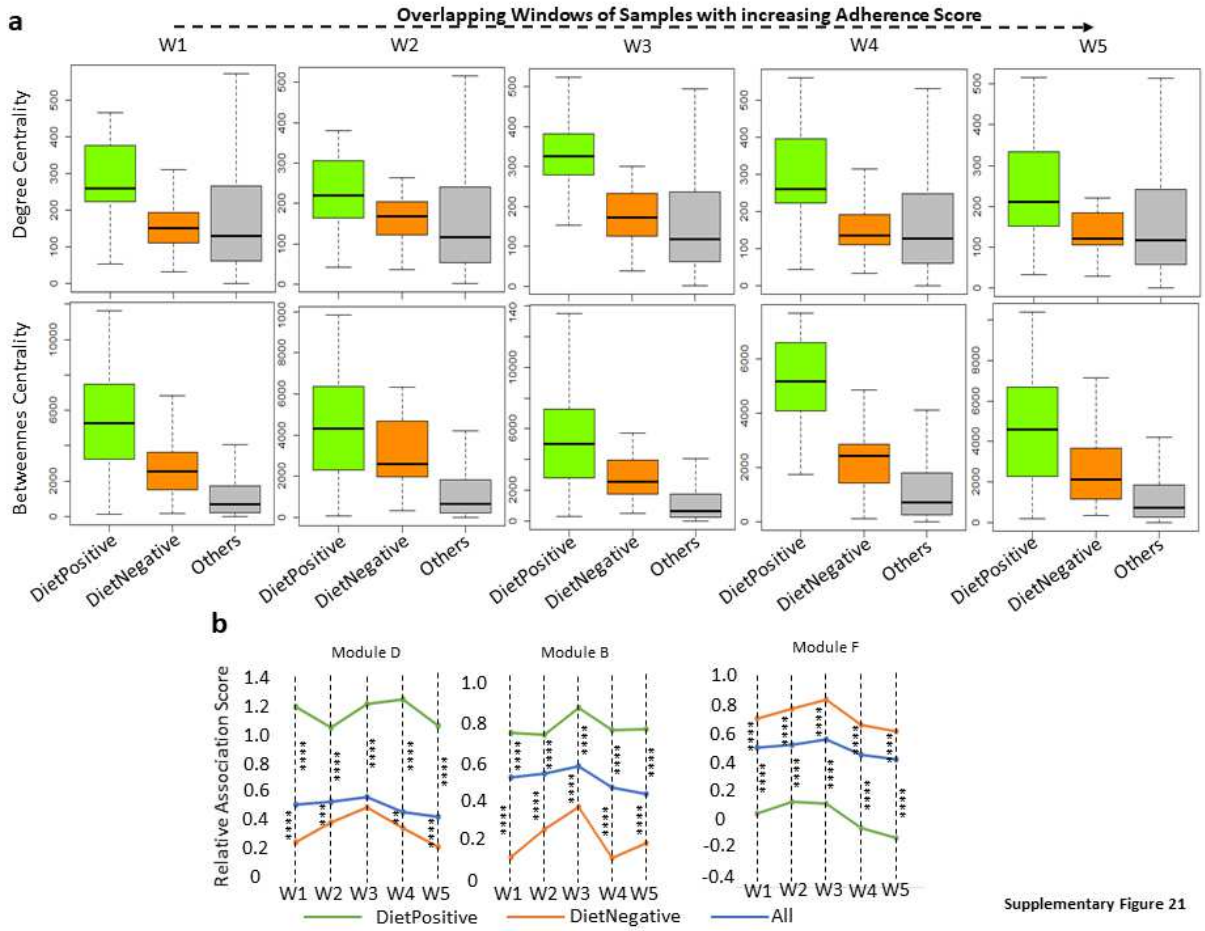

Supplementary Figure 21: a. Variation of the degree and betweenness centrality of the different groups of taxa across individuals belonging to the overlapping groups of increasing diet adherence scores. b. Relative co-occurrence propensities of the different groups of taxa with the iBBiG taxonomic modules. Relative co-occurrence propensities of the different groups with the frailty-associated Module C is provided in figure 5d.

SUPPLEMENTARY TEXT 3

COMPLETE DESCRIPTION OF METHODS USED FOR THE BIOINFORMATIC STATISTICAL ANALYSIS OF THE MICROBIOME DATA

Pre-processing of amplicon reads

The FLASH program was used to join the paired-end reads (25). The data was barcode-corrected and quality filtered using the QIIME package; followed by clustering of reads into Operational Taxonomic Units (OTUs) (97% identity threshold) using USEARCH Clustering algorithm; followed by chimeric removal (26, 27). The taxonomic classification of the representative sequences for each OTU was performed using both the RDP classifier (genus level: 0.8 confidence threshold) and the SPINGO classifier (species level: 0.7 confidence threshold) (28, 29).

Multi-variate analysis of dietary profiles and taxonomic profiles

Multivariate analyses using Principal Coordinate Analysis (PCoA) were performed using the ade4 package of the R programming interface, using Spearman distances of the individual sample profiles as well as the across time point changes (final-baseline).To test the significance of the between-country variation of the baseline dietary and microbiome profiles, Permutational Analysis of Variance (PERMANOVA) was performed on the PCoA objects using the adonis function of the vegan R package. Procrustes analysis was performed to quantify the relationships between the baseline diet and microbiome profiles using the procrustes function of the vegan package. The Shannon diversities of the samples were obtained using the diversity function of the vegan R package.

Machine Learning-based identification of microbiome taxa associated with the dietary intervention

The Machine learning based Random Forest (RF) approach (implemented in the randomForest package of R) was used to identify microbiome taxa significantly associated with NU-AGE FBDG adherence scores. We first divided individuals into three equal tertiles, namely ‘High Adherence’, ‘Medium Adherence’ and ‘Low Adherence’ in decreasing order of the change in adherence across time-points and the samples from each into two cohorts corresponding to the baseline and final time-points. Two separate models were created for the baseline and the final time points. The performance of the models was measured by calculating the correlation

between the actual and the predicted food scores obtained using the models. The RF approach provided the feature score importance scores for each microbiome component (OTUs) (indicating the extent of association of these with the dietary adherence scores). For identifying the most-predictive features, iterative random forest models (n=100, sample subset-size=100) with varying number of features (selected in decreasing order of their feature importance scores) were obtained using the randomForest package (two-fold cross validation) and their performances compared. Finally, to identify the OTUs associated with dietary adherence, a Reboot approach (using Spearman correlations) was used to identify OTUs that were significantly associated with adherence scores with an FDR corrected P-value < 1e-5 (30). OTUs positively and negatively associated with diet were classified as DietPositive and DietNegative, respectively. A pictorial representation of the workflow adopted for this entire step is provided in **Supplementary figure 1**.

Overview: iBBiG is based on the detection profile of the taxonomic units (in this case, the Operational Taxonomic Units (OTUs)). It then utilizes an iterative, heuristic, genetic-algorithm based methodology to identify modules of taxa within a microbial community that tend to show strong co-occurrence relationships across a given population of microbiomes. The primary advantage of this strategy is its flexibility, as it allows identification of over-lapping modules such that certain taxonomic units can be part of multiple modules. Such a partitioning strategy makes more biological sense as certain taxa (or species) can be part of multiple guilds because of their functional versatility or may be functionally specialized (i.e. belonging to specific guilds).

Method: For identifying modules within the gut microbiome, we used the **i**terative **B**inary **Bi**-clustering of **G**ene-sets (iBBiG) approach (38). Rather than profiling abundances or proportions, iBBiG investigates the detection profile of the taxonomic units or OTUs. Subsequently, an iterative, heuristic, genetic-algorithm based methodology is used to identify taxonomic modules that tend to show strong co-occurrence relationships across a given population of microbiomes. For performing the iBBiG based clustering, we used the iBBig function available within the Bioconductor package of R. While OTUs belonging to the different modules were then classified based on their clustering patterns, samples were classified based on the occurrence of the different iBBiG modules within them. The taxonomic compositional pattern of each module was then obtained by collating the RDP-based genus classification of each OTU and subsequently rank-normalizing these based on the abundance

of each genus (in terms of the number of OTUs) across a module. To associate the modules with frailty, we first obtained the frailty status of each individual at each time-point (0: Non Frail; 1: Pre Frail; 2: Frail). Subsequently based on the changes across time-points, individuals across the cohorts were classified as 'Reduced Frailty', 'No Change' and 'Increased Frailty'. The representation of each of the modules were obtained at both the time-points for each of three groups of individuals. The occurrence changes of each module (the number of samples in which a module is present at follow-up divided by the number of samples the module is present in at the baseline) were computed for each group. The log fold changes in these ratios in the Reduced Frailty with respect to the Increased frailty groups would provide the enrichment or depletion of the modules in individuals with reduced frailty as compared to those showing an increase in frailty across time-points. A positive change would indicate enrichment, and a negative value would indicate depletion. To compare the patterns across modules X and Y, Chi-square tests (using the chisq.test function of R) were then performed on the contingency tables containing four values, namely occurrence at baseline and follow-up of reduced frailty and occurrence at baseline and follow-up of increased frailty, corresponding to the two modules. To check for the significance of the differences of the occurrences across modules in terms of their diet association, we obtained number of times a module was present in the list of DietPositive and the DietNegative OTUs, and subsequently compared them using the Fishers' Exact test (fisher.test function of R).

Associating dietary adherence and microbiome changes with frailty and inflammation

For associating the abundances of the adherence associated marker OTUs with the different measures of frailty, cognitive function and cytokine profiles, we computed Spearman correlations using the corr.test function of the psych package in R (along with the Benjamini-Hochberg corrected p-values).

To account for various confounders, we used Partial Correlations (partial.r and the corr.p functions of the psych R package). Partial correlations measure the strength and the direction of the association between two variables considering the effect of confounding variable (s). Partial Correlations are like multiple regressions with confounders but not limited to specific distributions of the response and predictor variables. Further, one can compute rank-based non-parametric measures of association like the Spearman rho (which we have used in this study), after considering the confounding effect of other factors like adherence scores or age/BMI/gender.

Computation of Microbiome Indices

A pictorial representation of the methodology for this purpose is described in **Supplementary figure 2**. This scoring scheme 'rewards' samples with higher abundances of Marker OTUs with increasingly positive association with adherence scores and taxes those which have higher abundances of Marker OTUs with negative associations with adherence scores.

For each sample, the diet-modulated microbiome score was computed using the following formula:

$\sum_{\text{across all marker OTUs}}$ (OTU correlation with Diet adherence scores) * Abundance of the OTU

To avoid over-fitting, leave-one out strategy was applied where for computing the microbiome index for a given sample, the sample was not considered while calculating the OTU correlations (with Diet Adherence scores).

Obtaining Inferred Microbial Metabolite Profiles based on Species Abundance Profiles

Literature annotated Species-to-Metabolite consumption/production associations were already available as part of the Virtual Metabolic Human database as well as those obtained in a recent meta-analysis by Sung *et al* (32, 33). These were parsed to create a present/absence information map of around 300 metabolite production and consumption profiles in greater than 900 species in a 0 (absent) and 1 (present) notation. Given the SPINGO-based species abundance profile, from the 16S amplicon data, the inferred metabolite profile was then obtained as an inner product of the species abundance profile and the species-to-metabolite map.

Generation of co-occurrence networks and computation of centrality measures

We used the Reboot Approach for generating the inter-microbial co-occurrence/co-inhibition networks (30) (described in **Supplementary text 4**). The co-occurrence networks obtained were visualized using Cytoscape (34). For any network, two different centrality measures were calculated for the nodes, namely degree centrality and betweenness centrality using the igraph R package. The relative co-occurrence propensities between any two groups of taxa were calculated as the log of the number of positive edges divided by the number of negative edges.

Given any two features (in this case, the OTUs), the Reboot approach computes the association between the two features using two different distributions of association measures obtained using repeated iterations as described below(52). The association measure can be any score, like the Pearson correlation, Spearman correlation, the Regression coefficients, or even the effect size measures. The first distribution (bootstrap distribution) was obtained by taking the repeated sub-samples of randomly selected observations and then computing the

association between the two features. This profiled the association values across an entire observation landscape, thereby removing biases which could be present because of specific samples. The second distribution (null distribution) was obtained by performing an equal number of iterations, where in each iteration, a fixed set of values (which in this case was 50%) are swapped across samples for both the features. The profiles were then re-normalized and the associations computed for the two features. The distribution of the values obtained in the two distributions were then compared using any comparative tests (which in this case was Mann-Whitney). The p-values thus obtained were then False Discovery Rate (FDR) corrected (Benjamini-Hochberg) and those pairs of features having FDR-corrected associations of less than 1e-5 (threshold used in this study) were inferred to be significant and an edge drawn between them in the network. The directionality of the association was taken as the sign of the median value of the bootstrap distribution. While pairs of features with significant positive associations were used to create the co-occurrence network, those with negative associations were used to create the co-inhibition network.

*Please refer to the main document for the corresponding reference numbers.

Supplementary Table 2: List of top 129 OTU markers obtained using the Random Forest approach for the prediction of dietary compliance scores, along with their SPINGO classifications, association with food scores as well as the ranked feature importance scores for the baseline and followup time points

	Ranked Feature Correlation				
OTU	Baseline	Follow-up	Genus	Species	Final
OTU_4560	0.99412752	0.5041946	Unclassified	Unclassified	Unclassified
OTU_3114	0.98993289	0.9798658	Faecalibacterium	Faecalibacterium_prausnitzii	Faecalibacterium_prausnitzii
OTU_147	0.86996644	0.9941275	Unclassified	Unclassified	Unclassified
OTU_1205	0.95721477	0.9530201	Unclassified	Unclassified	Unclassified
OTU_300	0.96224832	0.9102349	Unclassified	Unclassified	Unclassified
OTU_584	0.98573826	0.9916107	Faecalibacterium	Faecalibacterium_prausnitzii	Faecalibacterium_prausnitzii
OTU_69	0.99832215	0.6526846	Unclassified	Unclassified	Unclassified
OTU_336	0.97986577	0.9781879	Roseburia	Unclassified	Roseburia_Unclassified
OTU_207	0.98238255	0.2332215	Unclassified	Unclassified	Unclassified
OTU_11233	0.2307047	0.9983221	Blautia	Ruminococcus_torques	Ruminococcus_torques
OTU_67	0.97651007	0.9974832	Unclassified	Unclassified	Unclassified
OTU_5978	0.98909396	0.658557	Unclassified	Unclassified	Unclassified
OTU_79	0.85151007	0.9899329	Eubacterium	Eubacterium_xylanophilum	Eubacterium_xylanophilum
OTU_131	0.90855705	0.9639262	Unclassified	Unclassified	Unclassified
OTU_1093	0.99496644	0.9211409	Anaerostipes	Unclassified	Anaerostipes_Unclassified
OTU_24	0.93875839	0.8557047	Unclassified	Unclassified	Unclassified
OTU_36	0.79026846	0.9630872	Prevotella	Prevotella_copri	Prevotella_copri
OTU_364	0.8909396	0.9513423	Clostridium	Clostridium_lactatifermentans	Clostridium_lactatifermentans
OTU_12121	0.95553691	0.8842282	Eubacterium	Eubacterium_eligens	Eubacterium_eligens
OTU_2352	0.95302013	0.1082215	Blautia	Unclassified	Blautia_Unclassified
OTU_1569	0.97902685	0.8213087	Clostridium	Unclassified	Clostridium_Unclassified
OTU_139	0.96979866	0.9991611	Clostridium	Unclassified	Clostridium_Unclassified
OTU_1006	0.41694631	0.9714765	Prevotella	Prevotella_copri	Prevotella_copri
OTU_1740	0.97147651	0.8708054	Unclassified	Unclassified	Unclassified
OTU_103	0.9295302	0.9437919	Unclassified	Unclassified	Unclassified
OTU_9966	0.97315436	0.7709732	Unclassified	Unclassified	Unclassified
OTU_8631	0.14177852	0.9446309	Prevotella	Prevotella_copri	Prevotella_copri
OTU_3603	0.68959732	0.9865772	Unclassified	Unclassified	Unclassified

OTU_1594	0.94211409	0.8011745	Eubacterium	Eubacterium_rectale	Eubacterium_rectale
OTU_32	0.98741611	0.9505034	Eubacterium	Eubacterium_eligens	Eubacterium_eligens
OTU_124	0.56459732	0.9731544	Unclassified	Unclassified	Unclassified
OTU_11498	0.23238255	0.989094	Anaerostipes	Anaerostipes_hadrus	Anaerostipes_hadrus
OTU_250	0.76090604	0.9790268	Unclassified	Unclassified	Unclassified
OTU_1221	0.95385906	0.9236577	Faecalibacterium	Faecalibacterium_prausnitzii	Faecalibacterium_prausnitzii
OTU_306	0.7533557	0.977349	Clostridium	Unclassified	Clostridium_Unclassified
OTU_120	0.9488255	0.4697987	Unclassified	Unclassified	Unclassified
OTU_1069	0.9647651	0.9966443	Clostridium	Clostridium_disporicum	Clostridium_disporicum
OTU_30	0.93791946	0.9127517	Clostridium	Clostridium_ruminantium	Clostridium_ruminantium
OTU_11429	0.97399329	0.7927852	Blautia	Unclassified	Blautia_Unclassified
OTU_8606	0.50838926	0.9572148	Unclassified	Unclassified	Unclassified
OTU_233	0.84563758	0.9463087	Eggerthella	Eggerthella_lenta	Eggerthella_lenta
OTU_6577	0.88255034	0.9488255	Blautia	Blautia_faecis	Blautia_faecis
OTU_64	0.77097315	0.9924497	Clostridium	Unclassified	Clostridium_Unclassified
OTU_86	0.92785235	0.9412752	Bacteroides	Bacteroides_thetaiotaomicron	Bacteroides_thetaiotaomicron
OTU_273	0.59647651	0.9689597	Clostridium	Unclassified	Clostridium_Unclassified
OTU_1280	0.94295302	0.2944631	Coprococcus	Coprococcus_catus	Coprococcus_catus
OTU_144	0.51677852	0.9521812	Parabacteroides	Unclassified	Unclassified
OTU_3372	0.70469799	0.9555369	Ruminococcus	Ruminococcus_bromii	Ruminococcus_bromii
OTU_12119	0.98322148	0.6417785	Unclassified	Unclassified	Unclassified
OTU_4016	0.94798658	0.3011745	Unclassified	Unclassified	Unclassified
OTU_6257	0.89597315	0.9379195	Roseburia	Roseburia_hominis	Roseburia_hominis
OTU_2604	0.96057047	0.8808725	Blautia	Blautia_faecis	Blautia_faecis
OTU_3860	0.94043624	0.817953	Blautia	Ruminococcus_obeum	Ruminococcus_obeum
OTU_470	0.97231544	0.4010067	Unclassified	Unclassified	Unclassified
OTU_21	0.96560403	0.965604	Anaerostipes	Anaerostipes_hadrus	Anaerostipes_hadrus
OTU_109	0.97483221	0.8372483	Clostridium	Clostridium_leptum	Clostridium_leptum
OTU_105	0.95637584	0.909396	Barnesiella	Barnesiella_intestinihominis	Barnesiella_intestinihominis
OTU_195	0.94379195	0.8833893	Unclassified	Unclassified	Unclassified
OTU_3501	0.55201342	0.9932886	Clostridium	Unclassified	Clostridium_Unclassified
OTU_9359	0.87248322	0.9387584	Faecalibacterium	Faecalibacterium_prausnitzii	Faecalibacterium_prausnitzii
OTU_168	0.87332215	0.9706376	Unclassified	Unclassified	Unclassified

OTU_3985	0.97063758	0.9110738	Faecalibacterium	Faecalibacterium_prausnitzii	Faecalibacterium_prausnitzii
OTU_34	0.9614094	0.8598993	Eubacterium	Eubacterium_hallii	Eubacterium_hallii
OTU_1356	0.73657718	0.9681208	Unclassified	Unclassified	Unclassified
OTU_5591	0.95050336	0.7063758	Unclassified	Unclassified	Unclassified
OTU_704	0.88422819	0.9404362	Unclassified	Unclassified	Unclassified
OTU_57	0.93959732	0.9244966	Eubacterium	Eubacterium_desmolans	Eubacterium_desmolans
OTU_16	0.96895973	0.9312081	Bifidobacterium	Bifidobacterium_longum	Bifidobacterium_longum
OTU_4302	0.96812081	0.8364094	Bifidobacterium	Bifidobacterium_longum	Bifidobacterium_longum
OTU_952	0.97567114	0.7206376	Eubacterium	Unclassified	Eubacterium_Unclassified
OTU_179	0.96644295	0.1635906	Unclassified	Unclassified	Unclassified
OTU_263	0.84647651	0.9614094	Veillonella	Veillonella_dispar	Veillonella_dispar
OTU_789	0.9840604	0.4572148	Parabacteroides	Parabacteroides_distasonis	Parabacteroides_distasonis
OTU_695	0.94714765	0.7986577	Blautia	Unclassified	Blautia_Unclassified
OTU_49	0.64765101	0.9395973	Eubacterium	Eubacterium_siraeum	Eubacterium_siraeum
OTU_178	0.9454698	0.9723154	Unclassified	Unclassified	Unclassified
OTU_152	0.9807047	0.738255	Unclassified	Unclassified	Unclassified
OTU_7093	0.55033557	0.9597315	Unclassified	Unclassified	Unclassified
OTU_2056	0.88842282	0.9823826	Unclassified	Unclassified	Unclassified
OTU_6936	0.01510067	0.9907718	Unclassified	Unclassified	Unclassified
OTU_1034	0.57969799	0.9496644	Unclassified	Unclassified	Unclassified
OTU_2345	0.65604027	0.9739933	Unclassified	Unclassified	Unclassified
OTU_1	0.85234899	0.942953	Eubacterium	Eubacterium_rectale	Eubacterium_rectale
OTU_4661	0.95889262	0.8473154	Clostridium	Unclassified	Clostridium_Unclassified
OTU_1914	0.36577181	0.9647651	Clostridium	Unclassified	Clostridium_Unclassified
OTU_98	0.86157718	0.9471477	Clostridium	Unclassified	Clostridium_Unclassified
OTU_1621	1	0.9169463	Unclassified	Unclassified	Unclassified
OTU_7618	0.96728188	0.7994966	Blautia	Blautia_faecis	Blautia_faecis
OTU_89	0.9135906	0.9538591	Eubacterium	Eubacterium_ventriosum	Eubacterium_ventriosum
OTU_162	0.89848993	0.9848993	Flavonifractor	Flavonifractor_plautii	Flavonifractor_plautii
OTU_45	0.94630872	0.9840604	Clostridium	Unclassified	Clostridium_Unclassified
OTU_287	0.94966443	0.7718121	Unclassified	Unclassified	Unclassified
OTU_23	0.90520134	0.9672819	Clostridium	Clostridium_ramosum	Clostridium_ramosum
OTU_11	0.87080537	0.9421141	Blautia	Blautia_luti	Blautia_luti

OTU_10307	0.96308725	0.7583893	Clostridium	Unclassified	Clostridium_Unclassified
OTU_22	0.89765101	0.9765101	Ruminococcus	Unclassified	Ruminococcus_Unclassified
OTU_1582	0.8716443	0.9454698	Unclassified	Unclassified	Unclassified
OTU_9740	0.38926174	0.954698	Unclassified	Unclassified	Unclassified
OTU_307	0.74412752	0.9479866	Clostridium	Unclassified	Clostridium_Unclassified
OTU_384	0.60067114	0.9815436	Unclassified	Unclassified	Unclassified
OTU_347	0.87416107	0.9857383	Clostridium	Unclassified	Clostridium_Unclassified
OTU_84	0.86493289	0.9832215	Unclassified	Unclassified	Unclassified
OTU_2336	0.95973154	0.7625839	Blautia	Unclassified	Blautia_Unclassified
OTU_4369	0.60151007	0.9563758	Clostridium	Clostridium_aldenense	Clostridium_aldenense
OTU_65	0.88674497	0.9580537	Unclassified	Unclassified	Unclassified
OTU_719	0.94127517	0.7365772	Clostridium	Unclassified	Clostridium_Unclassified
OTU_414	0.34312081	0.9605705	Mogibacterium	Unclassified	Mogibacterium_Unclassified
OTU_5014	0.98489933	0.9697987	Blautia	Ruminococcus_torques	Ruminococcus_torques
OTU_5819	0.94463087	0.7197987	Clostridium	Clostridium_sporosphaeroides	Clostridium_sporosphaeroides
OTU_125	0.9966443	0.454698	Unclassified	Unclassified	Unclassified
OTU_10029	0.76677852	0.9622483	Unclassified	Unclassified	Unclassified
OTU_5862	0.97734899	0.579698	Actinomyces	Actinomyces_lingnae	Actinomyces_lingnae
OTU_945	0.85067114	0.9807047	Unclassified	Unclassified	Unclassified
OTU_447	0.99580537	0.9152685	Unclassified	Unclassified	Unclassified
OTU_375	0.95469799	0.7919463	Clostridium	Clostridium_methylpentosum	Clostridium_methylpentosum
OTU_1637	0.99244966	0.8733221	Unclassified	Unclassified	Unclassified
OTU_11425	0.96392617	0.3833893	Blautia	Ruminococcus_torques	Ruminococcus_torques
OTU_8952	0.98825503	0.9874161	Coprococcus	Coprococcus_comes	Coprococcus_comes
OTU_291	0.95134228	0.9958054	Collinsella	Collinsella_aerofaciens	Collinsella_aerofaciens
OTU_52	0.98657718	0.966443	Eubacterium	Eubacterium_ramulus	Eubacterium_ramulus
OTU_3602	0.95218121	0.9161074	Unclassified	Unclassified	Unclassified
OTU_10880	0.95805369	0.8716443	Blautia	Unclassified	Blautia_Unclassified
OTU_14	0.98154362	1	Collinsella	Collinsella_aerofaciens	Collinsella_aerofaciens
OTU_27	0.97818792	0.9756711	Coprococcus	Coprococcus_comes	Coprococcus_comes
OTU_9293	0.99748322	0.9144295	Blautia	Ruminococcus_torques	Ruminococcus_torques
OTU_53	0.99077181	0.9949664	Blautia	Ruminococcus_torques	Ruminococcus_torques
OTU_1248	0.99161074	0.9588926	Unclassified	Unclassified	Unclassified

OTU_76	0.99916107	0.988255	Dorea	Dorea_formicigenerans	Dorea_formicigenerans
OTU_7369	0.99328859	0.9748322	Dorea	Dorea_formicigenerans	Dorea_formicigenerans

SUPPLEMENTARY TEXT 4

DIET-RESPONSIVE TAXA ARE NOT SPECIFIC TO NATIONALITY

We next checked if the diet-associated taxa differed across the nationalities. As noted above different nationalities were characterized by specific gut microbiome composition at baseline (**figure 1b; Supplementary figure 4a-b**) and different dietary adherence scores (Netherland and UK having significantly lower scores, followed by Italy with Poland and France having the highest) (**Supplementary figure 7a**) (as also reported by previous studies on this cohort) (18, 19). If nationality-specific differences in diet-associated taxa existed, the performance of the prediction models might vary across nationalities. However, despite differences in the baseline gut microbiome compositions, there was no significant difference in the performance of the model (mean squared errors) for the different nationalities except for Netherlands (where the error rate was significantly high) (**Supplementary figure 7b**). This indicates that the identified diet-associated taxa were similar across most of the nationalities. The higher error-rate for the Netherlands could either be a consequence of lower adherence scores or a different set of diet-responsive taxa in these individuals. We tested the latter possibility by creating two different versions of iterative Random Forest models (two-fold cross validation) for Dutch subjects at baseline. While one version was created by using only the 129 diet-associated markers, the second version was built upon all OTUs besides the diet-associated markers. We observed that the iterative models built using only the 129 diet-associated markers had significantly higher correlation and significantly lower mean squared errors as compared to those obtained using all OTUs besides the diet-associated taxa (**Supplementary figures 7c-d**). This indicated that the diet-responsive taxa were not specific to nationality.

SUPPLEMENTARY TEXT 5

VALIDATING THE ASSOCIATION OF THE DIET-RESPONSIVE TAXA WITHIN THE INTERVENTION AND CONTROL COHORTS AS WELL AS WITHIN INDIVIDUALS WITH VARYING ADHERENCE TO THE MED-DIET

There were 1224 microbiota datasets corresponding to 612 individuals having matched microbiome profiles for both the baseline and the follow-up time points. To further verify their association with the MedDiet adherence, we checked the variation of the relative abundances of these OTU-groups across an entire adherence landscape. For this we arranged the microbiota data (of the individuals) from the entire intervention study in increasing order of their adherence to the diet, and subsequently divided them into five equally sized overlapping windows (of increasing adherence scores; five overlapping windows of 204 samples with an overlap of 102 samples). Adopting such a window approach would illustrate the gradual transitions of specific changes across an entire adherence landscape (after eliminating variations caused due to specific samples). As expected, profiling the abundance variation of the two taxa groups across the windows identified a progressive increase of the DietPositive taxa (Kruskal Wallis H-test P-value < 5e-4) and a concomitant decrease of the DietNegative taxa (Kruskal Wallis H-test P-value < 3.2e-7) with increasing adherence to the Mediterranean diet (**Supplementary figure 8**). Performing this window-based analysis separately within the baseline and final time points also revealed the same pattern (**Supplementary figure 8)**. We then checked whether the positive and negative associations of the DietPositive and DietNegative taxa in the intervention cohort were also reflected in the across time-point (final to baseline) changes in dietary adherence. For each of the diet-associated markers (i.e. the OTUs), we computed the log fold change in the gain/loss ratios (the number of individuals in whom an OTU is more abundant across the time-points divided by the number of individuals in whom it is decreased) in the intervention cohort with respect to the control cohort. We observed that for the DietPositive taxa, the intervention to control log fold difference of the gain/loss ratios were positive (indicating that the changes were more positive in the intervention cohort as compared to the controls) and significantly higher (Mann-Whitney U test P < 1.3e-4) than those obtained for the DietNegative taxa which were negative (indicating a decrease

across time-points in the intervention cohort as compared to the controls) (**figure 2c**). To further profile the changes in the abundance of the markers across individuals with varying degrees of changes in their adherence to the diet, we divided them into three equal tertiles, namely 'High Adherence', 'Medium Adherence' and 'Low Adherence' in decreasing order of their change in adherence across time-points. The abundance changes of the two groups of markers (DietPositive and DietNegative) were then profiled across the three groups separately. As expected, while the DietPositive OTUs had a significantly positive change in the High Adherence as compared to the Low Adherence individuals, an exactly opposite trend was observed for the DietNegative markers (**figure 2d**). These findings suggest that the associations of the specific taxa with diet are stable across cohorts as well as across the changes between time-points.

SupplementaryTable3: Number of OTUs belonging to each iBBiG module along with the major genera (relative abundance greater than 1% after removing the unclassified OTUs within each module

iBBiG_Module	Number of OTUs	Major Genera
a	291	Lachnospiracea_incertae_sedis, Blautia, Clostridium_IV, Coprococcus, Bacteroides, Faecalibacterium, Roseburia, Oscillibacter, Gemmiger, Ruminococcus, Alistipes, Bifidobacterium, Dorea, Flavonifractor, Clostridium_XlVa, Clostridium_XI, Parabacteroides, Streptococcus
b	153	Clostridium_IV, Coprococcus, Lachnospiracea_incertae_sedis, Oscillibacter, Faecalibacterium, Sporobacter, Flavonifractor, Gemmiger, Prevotella, Acetanaerobacterium, Bacteroides, Blautia, Butyricimonas, Clostridium_XlVa, Clostridium_XlVb, Enterorhabdus, Erysipelotrichaceae_incertae_sedis, Haemophilus, Methanobrevibacter, Parasutterella, Pseudobutyrivibrio, Ruminococcus, Slackia
c	90	Clostridium_IV, Alistipes, Oscillibacter, Erysipelotrichaceae_incertae_sedis, Flavonifractor, Sporobacter, Gemmiger, Ruminococcus, Acetanaerobacterium, Anaerofilum, Asaccharobacter, Blautia, Clostridium_XlVa, Eggerthella, Gordonibacter, Pseudoflavonifractor, Roseburia
d	99	Lachnospiracea_incertae_sedis, Bacteroides, Blautia, Coprococcus, Faecalibacterium, Ruminococcus, Alistipes, Clostridium_XlVb, Gemmiger, Anaerostipes, Barnesiella, Butyricimonas, Clostridium_IV, Dorea, Haemophilus, Lactococcus, Oscillibacter, Parasutterella, Sporacetigenium
e	142	Lachnospiracea_incertae_sedis, Blautia, Roseburia, Clostridium_XlVa, Bacteroides, Dorea, Bifidobacterium, Actinomyces, Clostridium_IV, Coprococcus, Gemmiger, Streptococcus, Anaerostipes, Clostridium_XI, Clostridium_XVIII, Faecalibacterium, Flavonifractor, Ruminococcus
f	66	Lachnospiracea_incertae_sedis, Blautia, Clostridium_IV, Faecalibacterium, Ruminococcus, Actinomyces, Alistipes, Anaerostipes, Bacteroides, Clostridium_XlVa, Coprococcus, Dorea, Eggerthella, Erysipelotrichaceae_incertae_sedis, Flavonifractor, Gemmiger, Gordonibacter, Granulicatella, Rothia

Supplementary Table 4: Number of samples classified to various iBBiG modules

iBBiG Modules	Number of Samples
a	1236
b	420
d	294
c	262
f	65
e	44

SUPPLEMENTARY TEXT 6

RESULTS OF THE APPLICATION OF THE iBBiG APPROACH ON THE NU-AGE DATASET

The application of the iBBiG approach on the NU-AGE data identified 6 overlapping taxonomic modules that had a high mutual co-occurrence (obtained by maximizing the internal entropy) within the dataset. These were referred to as modules 'A' to 'F' (**Supplementary figure 9a**). Based on their detection trends in the overlapping modules, the OTUs could be classified as belonging to either a single (e.g. module A) or a combination of any of the six modules. This resulted in 36 OTU classifications (including one 'not classified' group). In a similar manner, a given sample could be classified into one of 15 classifications (and one 'not classified' group) based on the detection of the various modules in that sample. The classifications of each OTU and sample obtained in the iBBiG approach is listed in **Supplementary Tables 3 and 4**. Each of the six modules were characterized by different number of OTUs, specific trends of prevalence across individuals, as well as distinct patterns of taxonomic composition (**Supplementary figures 9b-c**). We also identified differential associations of each of these modules with frailty, especially with modules B and D being significantly enriched in the individuals with reduced frailty from baseline to post intervention, as compared to the module C, which was enriched in those with increasing frailty (**Supplementary figures 9d**). This indicates module 'C' to be similar to the long-stay-like modules we identified in ELDERMET individuals using the iBBiG approach(16). However, module 'C was not only associated with a significant enrichment in individuals with increased frailty, but also an increase in representation of the set of DietNegative OTUs (**Supplementary figure 9d**). The observation that adherence to the diet could specifically select against taxa associated with frailty indicates the likelihood that the Mediterranean diet successfully modulated the gut microbiome in a manner predicted to be negatively associated with frailty. A major objective of the NU-AGE dietary intervention was the reduction of frailty and inflamm-ageing in the elderly. Therefore, we next investigated in detail the association of adherence-associated taxa with frailty as well as with the inflammation status of the individuals.

SUPPLEMENTARY TEXT 7

ACROSS TIME-POINT CHANGES OF THE DIET-RESPONSIVE TAXA IN INDIVIDUALS WITH VARIED CHANGES IN THEIR FRAILTY STATUS

Based on the changes in their frailty status across time-points, the individuals across the cohort could be divided into three groups, namely those with 'Reduced Frailty', 'No change in frailty' and 'Increased Frailty'. We then investigated the across time-point changes in these taxa. To measure whether the above trends were also reflected in the across time-point changes, for each OTU, we computed the effect-size of the time-point changes between the individuals with reduced frailty as compared to the other two groups (**See Methods**). A positive effect size change would indicate that the taxa show more positive change (that is either an increase or a relative lower decrease) in their abundance across time-points in individuals with reduced frailty (as compared to those with no change or increase in frailty), and vice-versa. In this regard, while the diet-enriched (that is the DietPositive) taxa showed significantly positive changes in the individuals with reduced frailty (as compared to the other two groups), the DietNegative group showed the opposite trend (**Supplementary figure 10b**). These findings further affirm our earlier observation of the depletion of the specific frailty-associated iBBiG module 'C' which was observed to have a negative association with diet as well as the notable increase of frail individuals in the control group. In line with these observations, in the control group, we observed a marginally significant increase (as compared to the intervention group) during the intervention period in the proportion of individuals with increased frailty (Fishers' Test $P < 0.06$; **Supplementary figure 10c**).

Supplementary Table 5: List of A) Frailty and Cognitive Function associated measures and B) Cytokines used for performing association analysis with the diet modulated microbiome components.

(A)

Category	Measure	Description	Directionality
Physical Frailty	Hand Grip Strength	Mean hand grip strength of the dominant hand (3 trials)	Negatively associated with frailty
	Gait Speed (Fastest time)	Gait Speed Fastest Time taken (2 trials)	Positively associated with frailty
	Fried Score	Fried Score for computing frailty	Positively associated with frailty
Cognitive Functioning	Geriatric Depression Score	Score for measuring geriatric depression (higher values indicate depression)	Negatively associated with cognitive function
	MMSE	Mini Mental State Examination (Scores range 0-30). Higher scores indicate better cognitive function	Positively associated with cognitive function
	BabCok Memory Score	Bab Cock Score for immediate recall	Positively associated with cognitive function
	CAMDEX-Q Scores	Cambridge Examination of Mental Disorders	Positively associated with cognitive function
	Constructional Praxis	CERAD Battery Total Score on Constructional Praxis	Positively associated with cognitive function
	Verbal Fluency	CERAD Battery Total Score on Verbal Fluency Categories	Positively associated with cognitive function

(B)

Cytokines
IL-13
Pentraxin-3
Adiponectin
TNF-A
G-CSF
IL-8
Ghrelin
IL-6
Resistin
hsCRP

IL-1b
TGF-b1
IL-4
IL-17
IL-1ra
IL-2
Leptin
sTNF-R1
IFN-g
IL-7
IL-12 p70
sGP130
GM-CSF
IL-5
sIL-6ra
MIP-1b
IL-10
MCP-1-MCAF
IL-18
sTNF-R2
IL-17a

SUPPLEMENTARY TEXT 8

ASSOCIATION OF MICROBIOME INDEX WITH THE DIFFERENT DIETARY COMPONENTS

Next, given that we calculated the microbiome index as a single value index providing a quantitative summary of the abundance patterns of the diet-associated markers (the higher the value, the higher the abundance of Diet-Positive taxa and the lower the abundance of Diet-Negative taxa, and vice-versa), as a sanity-check, it is important to validate that the calculated microbiome index captured the association patterns of the individual diet-associated marker OTUs. For this, we repeated the analysis performed earlier for the individual marker OTUs (**Supplementary figure 12**) on the overall microbiome index (after adjustment for confounders) (**Supplementary figure 13**).

SUPPLEMENTARY TEXT 9

ASSOCIATION OF DIET-ASSOCIATED MICROBIOME TAXA WITH DISEASE PATHOPHYSIOLOGIES, POLY-PHARMACY, AND OTHER HOST-FACTORS

The dataset included 11 diseases containing at least three (of 612) diseased subjects at the baseline. We first investigated the effect of these diseases on the diet-associated taxa at the baseline. Nine of the 11 diseases were associated with lower microbiome indices, significantly so for diabetes, heart attack and inflammatory disorders ($P < 0.05$) and marginally significant for Cancer ($P < 0.097$) (**Supplementary table 6**; **Supplementary figure 14 a-d**). Individuals with multiple diseases had significantly lower microbiome indices and significantly lower ratios of DietPositive to DietNegative taxa abundances compared to those with single or no disease, indicating that the diet-favoured microbiome components are negatively associated with disease at baseline (**Supplementary figure 14e-f**). However, when we examined partial spearman correlations at baseline, the pattern of association of microbiome index with seven of the 10 inflammatory markers and frailty indices (identified in **figure 4**) remained invariant even after taking into account all confounders including age, BMI, gender, poly-pharmacy and different disease pathophysiologies (**Supplementary figure 15a**). All the above associations were retained (except for leptin) even after considering age, gender, BMI and poly-pharmacy (as confounders) across both the baseline and follow-up time points, further supporting the hypothesis that it is the microbiome response that is linked to the above measures (even after adjusting for all host associated confounding factors) rather than dietary adherence alone (**Supplementary figure 15b**).

SUPPLEMENTARY TEXT 10

ASSOCIATION OF CHANGES (BETWEEN THE FINAL AND BASELINE TIME-POINTS) IN MICROBIOME INDEX WITH DIFFERENT MEASURES.

To further illustrate the links between diet, microbiome, and health, we investigated the associations of the across time-point changes of the various measures with the change in diet and microbiome. The change in microbiome index was not associated with either baseline dietary adherence scores (linear regression R=-0.034; $P < 0.31$) or the 12-month dietary adherence scores (linear regression R = 0.05; $P < 0.12$) (**Supplementary figure 15a, b**). We first performed an in-depth investigation of the association of the across-time-point (follow-up to baseline) changes in cytokine levels for each individual with the corresponding change in microbiome indices. Cumulated levels of anti-inflammatory cytokines were calculated as the summed ranked abundances of the anti-inflammatory cytokines (IL-10, IL-4, IL-5 and IL-1ra). Ratio of hsCRP levels to anti-inflammatory cytokine levels was calculated as the ratio of the ranked abundance of hsCRP to the cumulated levels of anti-inflammatory cytokines (calculated as above). Then for each cytokine (or cytokine ratio), the changes were calculated as the differences in levels between the follow-up and the baseline time-points. For inflammatory markers like hsCRP, MCP1-MCAF, Resistin, positive changes in microbiome indices were associated with significant negative changes in the levels of these cytokines (**Supplementary figure 15c**). For other inflammatory cytokines like IL-17, IL-6, MIP-1b, etc, the associations were still negative, although not significant. An exact opposite trend was observed for the anti-inflammatory cytokine IL-10, where positive changes in microbiome indices were associated with significant positive changes in the levels of this cytokine. As a consequence, positive changes in microbiome indices were associated with negative changes in the hsCRP to anti-inflammatory cytokine levels (**Supplementary figure 15c**).

Additionally, a pairwise regression approach was also used to identify associations between microbiome response, adherence score changes and the identified measures of frailty, cognitive function and inflammation. Given any two measures, we performed linear regressions of the measures with each of the scores using country and age as confounders. We did not use FDR correction at this stage as we were investigating associations with specific measures. Linear relationships with P-values less than 0.05 and between 0.1 and 0.05 were identified as being significant and trend, respectively.

The significant associations identified from this analysis are illustrated in **Supplementary figure 15d)** As expected, microbiome response was positively associated with dietary adherence changes. However, it was this increased microbiome response that displayed positive associations with reduced frailty (Reduced Fried Score), improved cognitive function (BabCock Memory Score) and negative associations with inflammation (hsCRP and another pro-inflammatory marker MIP-1b). The adherence score change, by itself, did not have any significant association (with exception of a negative association with MIP-1b). The above results clarify the relationships between diet, microbiome and improved life-status. Change in adherence (that is increasing adherence to a Mediterranean diet) is likely to modulate specific components of the microbiome. It is this microbiome response, when induced, that is associated with reduced frailty and reduced inflammation. However, at each interaction point, there may be exceptions.

Supplementary Table 6: A. Number of subjects with gut microbiome profiles at baseline that belong to the different disease categories (no_disease refers to those individuals who were not identified with any disease symptoms). B. Results of the Mann-Whitney test based comparative analysis of the diet-associated microbiome indices for the individuals with different diseases with control (no_disease type) individuals at baseline

(A)

Disease_Type	Number of Subjects
no_disease	324
high_cholesterol	183
thyroid	61
diabetes	30
cancer	27
hypertension	21
food_allergy	15
respiratory_disease	14
swollen_ankle	10
kidney_disease	6
heart_disease	5
inflammation	3

(B)

	Diet-Associated Microbiome Index	
Disease Type	Direction	Mann-Whitney P-value
hypertension	Lower In Disease	0.005346
diabetes	Lower In Disease	0.005646
inflammation	Lower In Disease	0.02727
cancer	Lower In Disease	0.097
respiratory_disease	Lower In Disease	0.1642
food_allergy	Lower In Disease	0.2569
swollen_ankle	Lower In Disease	0.3086
heart_disease	Lower In Disease	0.3212
high_cholesterol	Lower In Disease	0.4621
kidney_disease	Higher In Disease	0.7945
thyroid	Higher In Disease	0.8938